THE UNIVERSITY OF MANITOBA

TORQUE BEHAVIOUR OF INDUCTION-TYPE RELAYS WHEN SUBJECTED TO HARMONICALLY DISTORTED WAVE FORMS

by

D. E. SARAMAGA

A THESIS

SUBMITTED TO THE FACULTY OF GRADUATE STUDIES

IN PARTIAL FULFILMENT OF THE REQUIREMENTS FOR THE DEGREE

OF MASTER OF SCIENCE

DEPARTMENT OF ELECTRICAL ENGINEERING

WINNIPEG, MANITOBA

May 1972

ACKNOWLEDGEMENT

The author wishes to acknowledge his indebtedness to Professor G.W. Swift for his continuing interest, guidance and assistance in carrying out this work. The assistance of Manitoba Hydro in providing facilities and equipment for some of the practical measurements is also acknowledged.

ABSTRACT

The object of this thesis was to investigate the torque behaviour of induction-type protective relays when subjected to harmonically distorted wave forms with a view to predicting variations from their published fundamental frequency operating characteristics.

The harmonic content supplied by large scale HVDC transmission converters was taken as the starting point for surveying the response of typical induction disk protective relays. This was extended to include the frequency response characteristics of these same devices.

The theoretical analysis of torque production was extended by considering the effect of varying the frequency of the operating quantities. This was then related to performance under conditions of harmonic distortion so that significance of this distortion can be determined.

TABLE OF CONTENTS

LIST OF ILLUSTRATIONS

CHAPTER 1

INTRODUCTION

The function of protective relaying as applied to ac power systems is to remove from service any element when it starts to operate in an abnormal manner that might cause damage or otherwise interfere with the effective operation of the rest of the power system or when the element itself is subjected to duty beyond its capability. These abnormal conditions may be the result of short circuits or they may be caused by overloading or overstressing of certain elements due to changing system steady state operating conditions or transient phenomenon.

The satisfactory application of the protection devices must take into account many diverse factors. The constraints to be satisfied include sensitivity, selectivity and reliability. The first of these is a measure of a relay device's ability to differentiate between the operating and non-operating condition. Selectivity refers to the ability of several in line relay devices to successfully sort out their sequence of operation so that the smallest possible portion of the system is removed from service. Reliability is a measure of the ability of a protective system to perform its duty according to a previously arranged plan.

Many types of relay devices are applied in conventional ac systems. Among the most common are relay devices based on the induction principle. Induction-type relays are essentially split-phase induction motors with contacts. Actuating force is developed in a moveable rotor element by the interaction of electromagnetic fluxes. Suitable restraining forces are provided to control the operating speed characteristics.

Due to the operating principles of induction-type relays it could naturally be expected that their characteristics would be affected by a change in frequency. This is because their synchronous speed, like that of induction motors would vary directly with frequency. Operating characteristic changes occurring with varying frequency have been recognized in the past with respect to generator pre-warming at low speeds and at overspeeds occurring during generator load rejections[9].

The introduction of HVDC converter stations and their associated generation of harmonics into the ac system introduces a completely new aspect to the application of conventional induction-type relays. It is the subject of this thesis to investigate the possible reprecussions of this harmonic content on conventional ac system induction-type relays.

CHAPTER 2

SOURCES OF HARMONIC DISTORTION

2.1 Normal Stray Harmonic Content of Ac Power System Wave Forms

Harmonic content in the normal wave forms of ac power systems is generally quite low. This is because the vast predominance of loads are linear-resistive in nature or consist of motors which have been specifically designed to remain linear over their normal operating range.

Nonlinear loads except for occasional large industrial rectifier installations are an extremely small factor. Typical values of harmonic content, measured at Harrow Substation on the Manitoba Hydro system, are given in Appendix A. The major harmonic component in the phase currents was the 5th which ranged in general from 1.5 to 3 percent of the fundamental.

2.2 Harmonic Content of Normal Ac System Fault Wave Forms

Except for initial spurious transient effects lasting perhaps a few cycles, relays are supplied with practically sinusoidal quantities under short-circuit conditions. This is because the short-circuit current is limited primarily by air-core reactance. This includes the leakage reactance of generators and transformers since their leakage flux is largely limited by an air path. Appendix B shows oscillographs of typical fault current wave forms which substantiate this point.

Unless saturation of their cores occurs, instrument transformers of conventional design are generally capable of reproducing these fault wave forms with good accuracy. Typically they are capable of maintaining ratio errors to less than a few percent for frequencies as high as 1500 Hz. Their overall performance is borne out by their accu-

rate response to the high frequency transients occurring in the early portion of the fault period. If saturation does occur so as to distort the applied primary wave form, as in overloaded current transformers for instance, it should only do so at high multiples of relay operating current in a properly designed application. This region of the relay characteristic will be shown later to be relatively independent of wave shape in any case.

2.3 Harmonic Distortion Introduced by Low-Voltage Testing

Errors introduced with so called phantom load or low-voltage testing of induction overcurrent relays have long been recognized. The effect is reviewed here for completeness since the underlying principles are closely related to the behaviour of induction relays with distorted wave forms applied. Further, it emphasizes that caution is necessary in any procedure set up to determine by test the effect of harmonic distortion in the applied wave shapes.

The effect follows from the fact that the relay impedance is not constant but varies as saturation proceeds. As shown in Figure 1a, when sine wave voltage is applied, sine wave current will flow up to the point where saturation begins. After this point the current increases faster than the voltage so that at 3.0 times the pickup voltage about 10 times the current will flow in this example. As seen in Figure 1b, the current wave will have a peak almost three times as high as if the ampere-volt curve were a straight line. Furthermore if the ammeter used happens to be a peak reading type calibrated to read rms current, it will read higher on the peaked wave form and so further distort the apparent results.

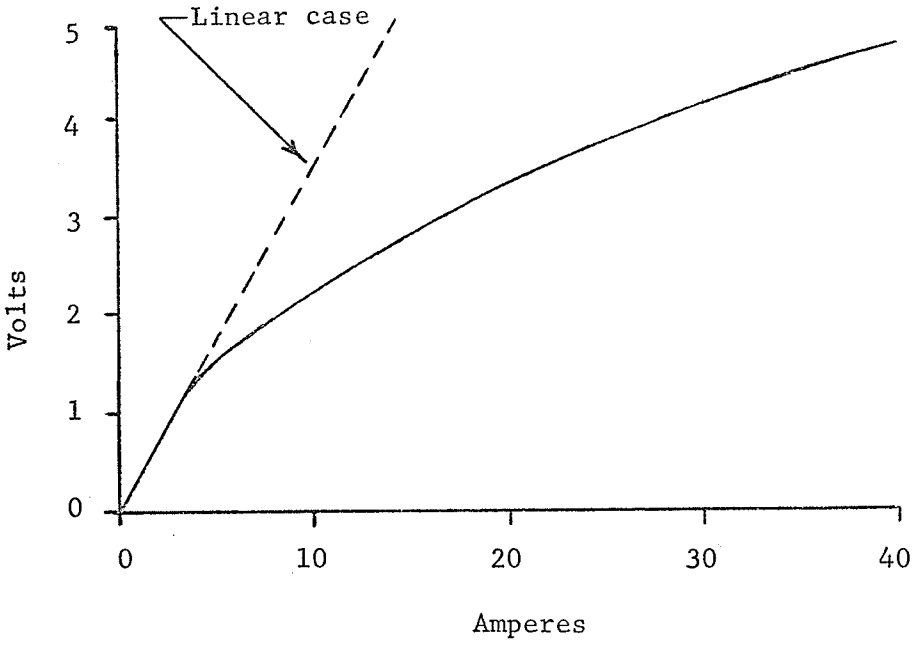

Figure 1a: Saturation curve of induction disk relay.

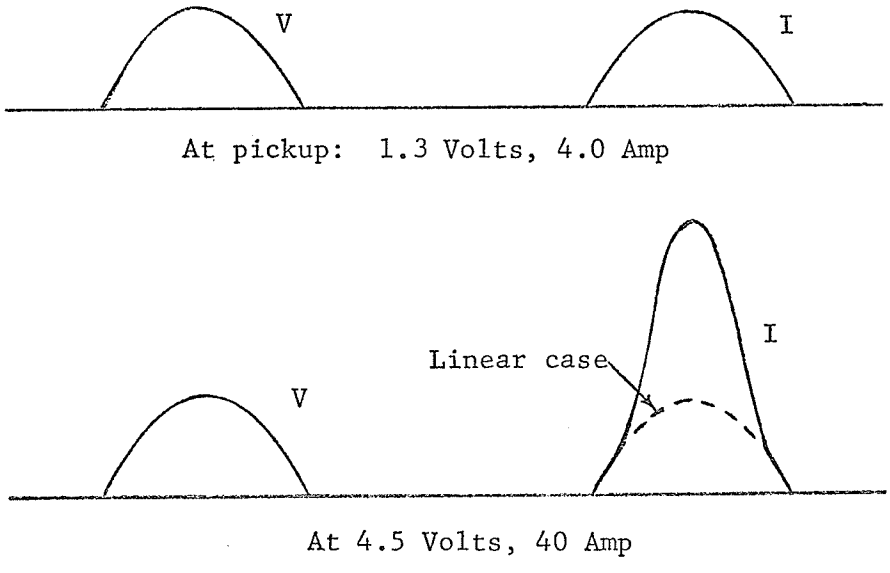

Figure 1b: Change in current wave form with saturation.

2.4 Harmonic Distortion Introduced by HVDC Transmission Schemes

2.4.1 Generation of Ac Harmonics

HVDC transmission schemes involve the introduction of large capacity rectifier and inverter installations to the existing ac systems. The connection of these converter devices, whether mercury arc or thyristor type, is extremely different from any other type of major ac system load. They are switching devices, the current wave shapes on the ac side being discontinuous but due to the large inductances on the dc side, having a flat top in the conducting regions.

The analysis of this periodic, nonsinusoidal current wave form provides the starting point for the somewhat complex question of harmonics. Figure 2 gives schematically an elementary circuit for a HVDC converter connection to an ac system utilizing the normal three phase full wave bridge connection. By considering the possible connections of the converter transformers and with appropriate degrees of assumption on behalf of the presence of circuit elements and control systems, the resulting wave shapes can be developed[1].

Figures 3a and 3b show the wave shapes of the ac line current for the cases of single bridge converters having star/star and delta/star transformer connections with winding ratios 1:1 and $\sqrt{3}$:1 respectively, with perfectly balanced three phase supply, zero commutation angle through neglecting commutation reactance and assuming infinite dc inductance or perfectly smoothed dc. Analysis of the wave shape is obtained from the Fourier Series:

$$i = a_o + \sum_{n=1}^{\infty} a_n \cos nwt + b_n \sin nwt$$

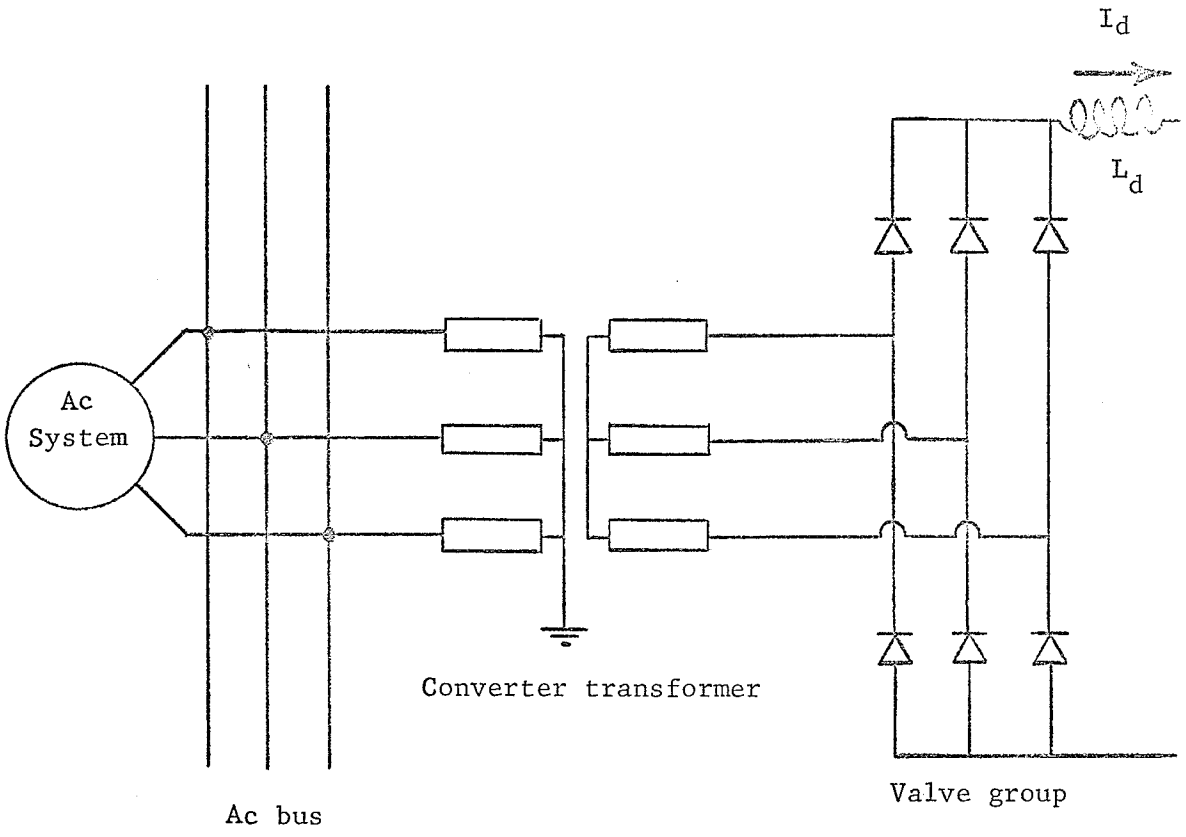

Figure 2: Connection of HVDC converter to ac system.

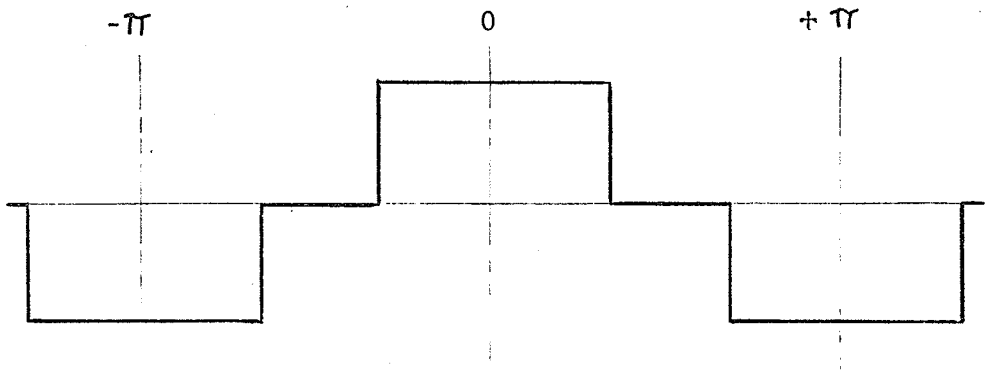

Figure 3a: Ac current wave shape with star/star converter transformer.

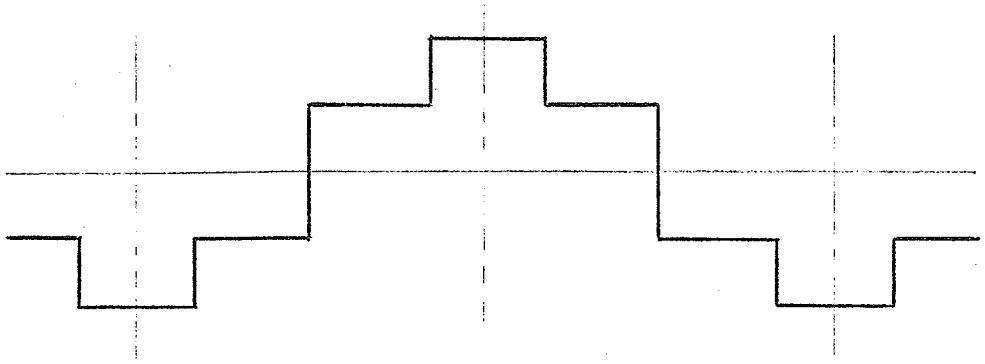

Figure 3b: Ac current wave shape with delta/star converter transformer.

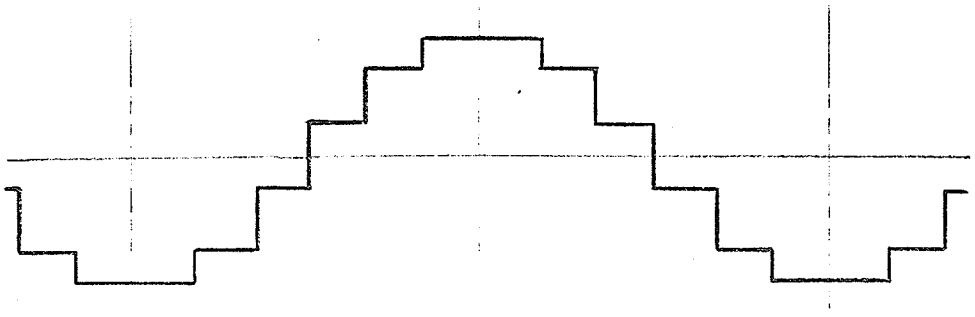

Figure 3c: Ac current wave shape for 12-pulse operation.

For star/star connected converter transformers and the above assumptions the solution for the ac line current is given by [1]:

$$i_o = \frac{2\sqrt{3}}{\pi} I_d \left[\cos wt - \frac{1}{5}\cos 5wt + \frac{1}{7}\cos 7wt - \frac{1}{11}\cos 11wt + \ldots \right.$$

$$\left. \ldots \pm \frac{1}{(6k\pm1)} \cos (6k\pm1)wt \ldots . \right]$$

where k is any integer.

For delta/star connected converter transformers and the same assumptions the solution for the ac line current is similarly given by:

$$i_o = \frac{2\sqrt{3}}{\pi} I_d \left[\cos wt + \frac{1}{5}\cos 5wt - \frac{1}{7}\cos 7wt - \frac{1}{11}\cos 11wt + \ldots \right.$$

$$\left. \ldots \pm \frac{1}{(6k\pm1)} \cos (6k\pm1) \quad \text{for k even} \right]$$

$$\ldots \mp \frac{1}{(6k\pm1)} \cos (6k\pm1) \quad \text{for k odd}$$

Thus with zero ac supply impedance and with symmetrical voltage wave forms, ac currents are square pulses consisting of fundamental component having rms value:

$$I_{(1)o} = \frac{\sqrt{6}}{\pi} I_d = 0.78\, I_d$$

and harmonics having rms values:

$$I_{(n)o} = \frac{I_{(1)}}{n}$$

These are of orders 5, 7, 11, 13 ... $6k\pm1$ with amplitudes 20, 14.3, 9.9, 7.7 ... percent of the fundamental frequency component.

When two bridges of equal capacity are working together either in series or in parallel, one with star/star connected transformer having winding ratio 2:1 and the other with delta/star connected transformer having winding ratio $2\sqrt{3}$:1, the resultant instantaneous current is given by the average sum of the equations for the individual connections:

$$i_o = \frac{2\sqrt{3}}{\pi} I_d \left[\cos wt - \frac{1}{11} \cos 11\ wt + \frac{1}{13} \cos 13\ wt - \frac{1}{23} \cos 23\ wt + \ldots \right]$$

$$\ldots \pm \frac{1}{6k \pm 1} \cos (6k \pm 1) \quad \text{for k even}$$

$$\ldots \text{ zero} \quad \text{for k odd}$$

This represents the output of a 12-pulse converter. The wave shape of the ac line current is shown in Figure 3c. Harmonic currents of orders 5, 7, 17, 19 will circulate between the two bridges, entering the ac system only if there is some unbalance between the two bridges.

In general the order of current harmonics introducted into the system by p-pulse converter operation will be:

$$n = kp \pm 1$$

where p is the number of pulse operation, an integer multiple of 6 for bridge type inverters having individual bridges displaced 360/p degrees from each other.

Theoretically an increase to 18, 24 or higher pulse operation is possible but it requires more expensive phase shifting transformers and becomes more dependent on circuit errors. The use of 12-pulse operation is therefore normally the most adaptable arrangement with 6-pulse operation retained for contingency conditions.

For the practical case the ac system and converter transformers

must be represented by a fundamental frequency voltage and a pure inductive reactance per phase. Including the effect of this commutating reactance results in current wave forms as shown in Figure 4 for a star/star connected transformer. The harmonic amplitudes[1] are now less than the maximums given above and depend on converter firing angles and commutation inductance. These harmonic currents comprise positive or negative sequence harmonics and can pass through transformers of any winding arrangement into the ac system.

The above discussion has been confined to symmetrical converter arrangements including accurate firing angles of all valves. In the event of asymmetry due to valve operation or inaccurate firing angles all other harmonics will be produced. These include positive or negative sequence systems of harmonic orders 2, 3, 4, 5, ... which can pass through the converter transformers into the ac system. High accuracy of valve operation and of firing angle generation by the control system is necessary to limit these quantities to insignificant values in operational systems.

2.4.2 Effect of Generated Harmonics on the Ac System

The generated harmonic currents enter the ac system and are distributed throughout it in accordance with the network impedances. Were measures not taken, these might penetrate the ac system radiating from the converter station, producing the likelihood of the following disturbing effects:

(a) Excessive harmonic currents in synchronous machines, power factor correction capacitors or other equipment.

(b) Overvoltages at points on the network.

(c) Interference in adjacent telecommunication lines.

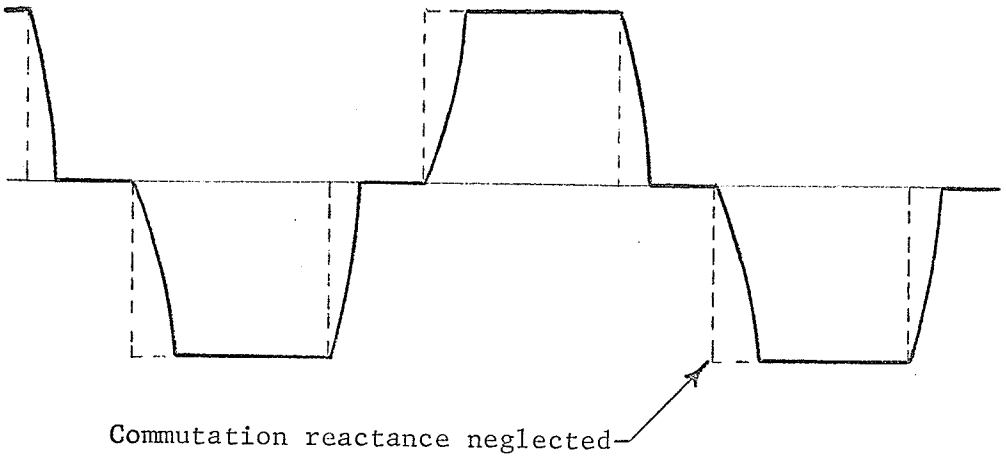

Figure 4: Ac current wave shape with commutation reactance considered.

(d) Interference with protective gear.

Unless the ac system is very large compared with the dc system suitable filtering is necessary to reduce the harmonic currents entering the ac system.

The filter configurations generally take the form of suitable arrangements of shunt filters attached to the ac busbars. It is thus possible to guarantee given values of harmonic voltages at this point regardless of ac system impedance variations. A typical filter configuration[3] employing single resonant arms in parallel for harmonic orders 5, 7, 11, 13 plus a low-pass filter arm for harmonic orders 17 and upwards is shown in Figure 5.

Unfortunately the configuration of harmonic filters on the converter terminals cannot guarantee harmonic voltage levels elsewhere in the system. In principle it is possible to calculate the harmonic voltages and currents at any point on the ac system. If acceptable levels of overvoltage, overheating and communications interference were defined, filter requirements could be solved accordingly. However there are great practical difficulties which include the following:

(a) De-tuning due to frequency variation from nominal system frequency can greatly affect the performance of high Q filters. This effect is particularly significant for cases of isolated generation feeding the dc system. Here frequency changes following load rejections can be particularly sizeable.

(b) Impedance parameters of lines, cables, etc., are never known to any great accuracy. At higher frequencies the capacative reactance becomes predominant. Some harmonics

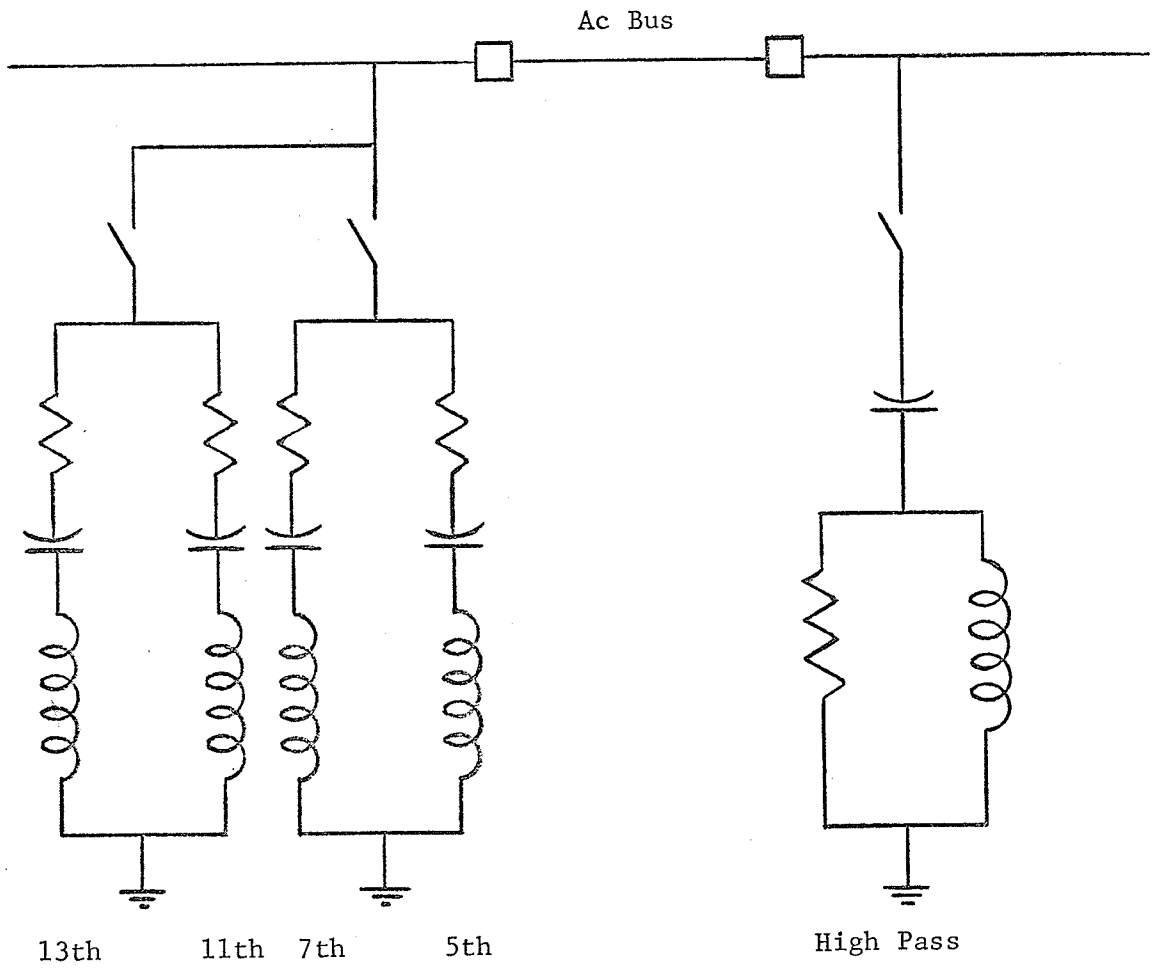

Figure 5: Typical ac harmonic filter configuration.

at whose frequencies resonances occur will be greatly amplified whereas others may be attenuated or surpressed.

(c) Configurations of most ac systems can change even over short periods due to switching of lines, generators, loads, etc. Harmonics may well excite other parts of the system to resonance in many and varied combinations. These may include series resonances of unloaded lines and transformers, parallel resonances of motor loads and shunt capacitance and propagation effects on transmission lines which become electrically very long at higher frequencies.

It is thus apparent that significant disturbing effects of harmonics are possible at points in the ac network connected to HVDC converters. This is so despite the usual provisions to limit the harmonic voltages to acceptable levels. Further, the disturbing effects are not necessarily confined to points near the converter station and in fact under unfortunate circumstances could occur randomly.

CHAPTER 3

DETERMINATION OF INDUCTION DISK RELAY CHARACTERISTICS WHEN EXPOSED TO HARMONIC DISTORTION OF OPERATING WAVE FORMS

3.1 Methods of Determining Quantitative Effects

That wave form errors and harmonic distortion of the operating quantities could effect the characteristics of induction-type relays has been qualitatively accepted for some time[6, 7]. However, these effects have held little significance prior to the introduction of large scale HVDC systems. For reasons which have been discussed in Section 2.1 and 2.2 the wave shapes supplied to the relays in normal ac system load and fault conditions have been sufficiently undistorted to permit confident application while presuming rated frequency conditions to apply in all cases. This approach also forms the basis of all classical theory of induction-type relays wherein the effects of frequency changes are neglected in the calculation of theoretical performance[8]. Where significant changes have been noted due to wave form distortion, such as in low voltage maintenance testing, the approach has been to remove the effect by changing to a more suitable procedure. In the latter example for instance, when resistive loading of a larger voltage source is used to control the current, the slight effect of wave form distortion introduced by the relay becomes negligible.

Accurate theoretical calculation of the operating characteristics is made extremely complicated by the various constraints involved in the overall torque production in a typical induction-type relay. These include the effect of the spring torques which control the pick-up values in the lower operating regions and saturation of the electromagnets to

produce definite minimum times in the higher operating regions. The total effect is to produce an irregular curve which follows no particular law. It was primarily for this reason that the design of induction-type relays with particular regard to their time characteristics has been one of trial and error in the past[11].

The most obvious approach to obtaining an accurate appreciation of the effect of harmonic distortion and related wave form errors on induction-type relays was therefore to undertake a series of practical tests designed to show these effects directly as changes in relay characteristics. This was done using current and voltage type induction disk relays which are in common usage on the Manitoba Hydro system.

3.2 Test Procedure for Obtaining Response to Harmonically Distorted Wave Shapes.

The test conditions were adopted on the basis of likely magnitudes and orientation of harmonic distortion to be introduced by HVDC converter stations into the ac network. These conditions have been shown earlier to be a probable cause of the most severe wave form distortion to be encountered by the relays under normal circumstances.

Characteristic current harmonics generated by the HVDC converter installations were shown in theory to be of the orders 5, 7, 11, 13, ... $kp\pm1$ with respective magnitudes approximately 20, 14.3, 9 .... $1/(kp\pm1)$ percent of the fundamental frequency component. Although suitable filtering is applied to maintain harmonic voltages at the converter ac buses to acceptable levels, it was also shown that normal system characteristics and operating conditions are conducive to a variety of resonance and propagation phenomenon which could result in significant magnification of these levels elsewhere in the ac system.

In order to determine quantitatively the possible effects of such harmonic distortion of the operating quantaties on the relay characteristics two basic tests were conducted:

(a) Harmonic distortion test - variations in relay operating time were observed while applying increasing amounts of harmonic distortion to the relay operating quantity. Tests included 5th, 7th and 11th harmonics of the fundamental 60 Hz wave form. Combinations of the applied harmonics were considered in some of the tests.

(b) Frequency response test - variations in minimum values of the relay operating quantity were observed for frequency changes from 50 Hz upward. By extending the frequency response test through the range of harmonic frequencies, performance under conditions of pure harmonic could be observed.

The test apparatus was set up as shown in Figure 6 for a typical overcurrent relay. The outputs of variable frequency sine wave oscillators were mixed via resistive pads and fed into a linear wide band power amplifier to produce the test wave shape supplied to the relay. An output transformer was used when current required for certain relays exceeded the current capability of the amplifier. In order to measure the effective value of current the instruments used were of the thermocouple or electrodynamic type, both being true rms movements.

The oscillators were not directly phase coupled but an attempt was made to minimize random drift by monitoring their outputs on an oscilloscope. This procedure was adequate for the purpose of these tests since even when drift was allowed to occur it did not cause variations

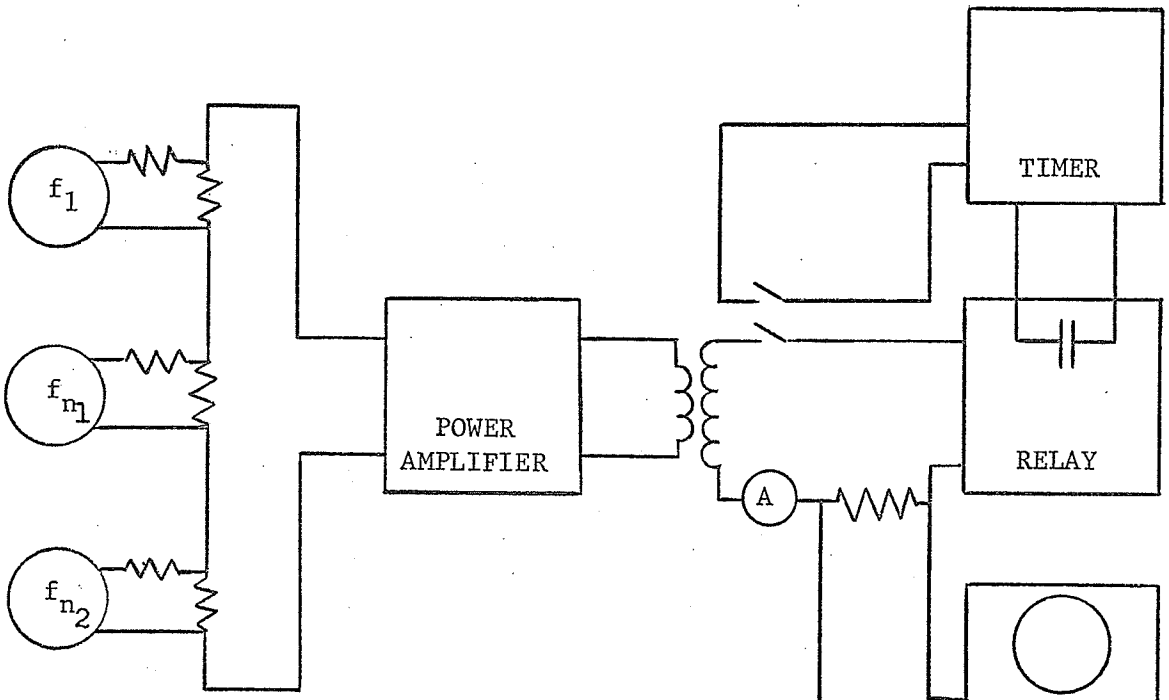

Figure 6: Test arrangement for determining effects of harmonically distorted wave shapes.

in the time measurements obtained.

3.3 Response of Relays to Distorted Wave Forms

Figures 7 to 16 give the results of the tests in the form of time characteristic curves and frequency response curves for each relay tested. The time characteristic curves include the effect of increasing harmonic distortion on the published characteristics. A brief summary of the findings for each relay is given:

3.3.1 IAC53 - Very Inverse Time Overcurrent Relay

From figures 7, 8a, 8b, 8c, 8d it is seen that operating time decreased fairly sharply with frequency between 40 Hz and 60 Hz with a minimum occurring in the 80 to 120 Hz range. Operating time then rose gradually with increasing frequency to 600 Hz. Variations were most pronounced at low multiples of tap value current. Adding even substantial amounts of harmonics (100 to 200 percent) produced only a minor change in characteristics with the relay operating slower.

3.3.2 IAC55 - Short Time Overcurrent Relay

From figures 9, 10a, 10b it is seen that operating time decreased with frequency between 50 Hz and 120 Hz and thereafter remained relatively constant to 600 Hz. Adding substantial amounts of harmonics (up to 100 percent) produced only a minor change in characteristics with the relay operating faster at low multiples of tap value current.

3.3.3 CO-8 - Inverse Time Overcurrent Relay

From figures 11, 12a, 12b it is seen that operating time decreased with frequency between 50 and 75 Hz and increased rapidly above 100 Hz. These variations were more pronounced for low multiples of tap value current. Frequencies above 180 Hz produced a reverse torque as evidenced by the relay resetting more rapidly when energized at these

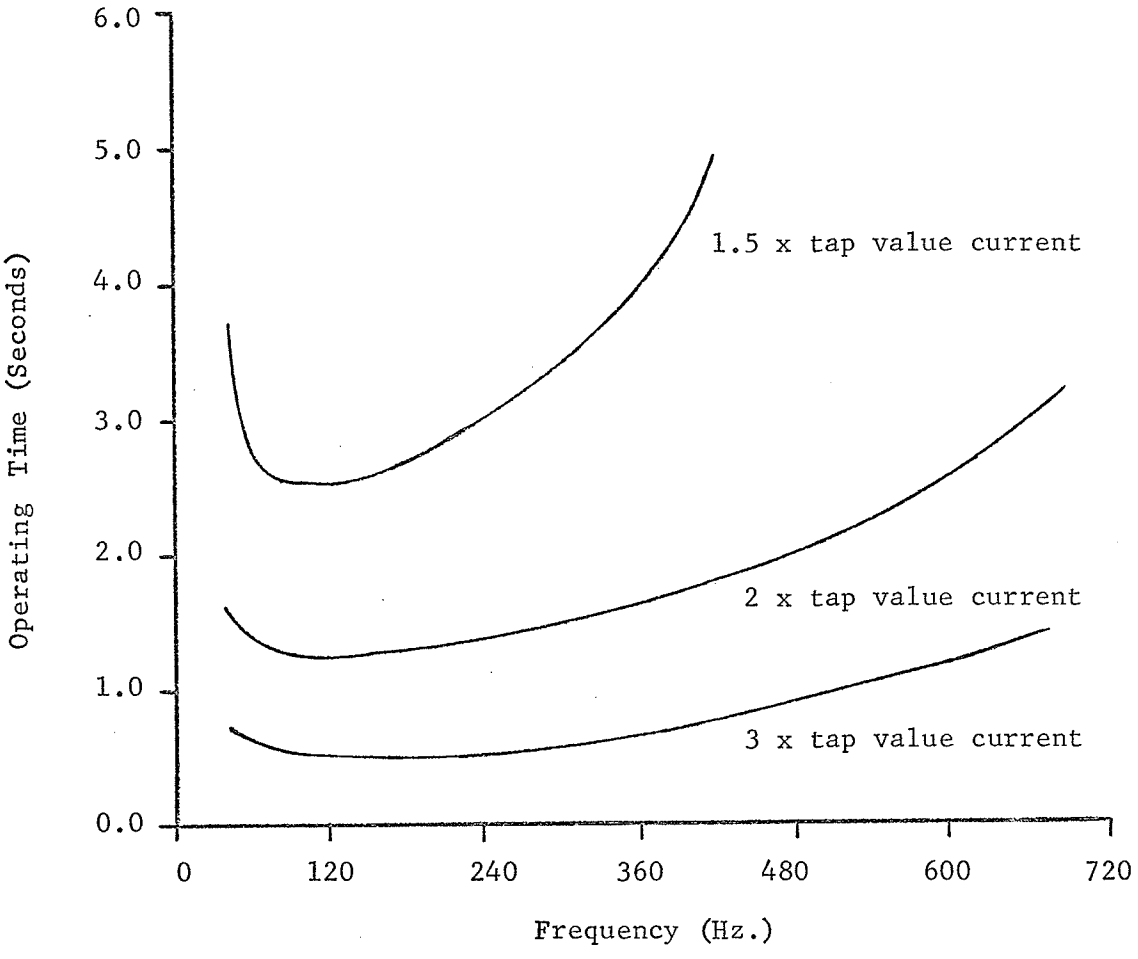

C.G.E. model IAC53A2A
Tap = 1.5 Amps
Time dial = 1

Figure 7: IAC53 frequency response characteristics.

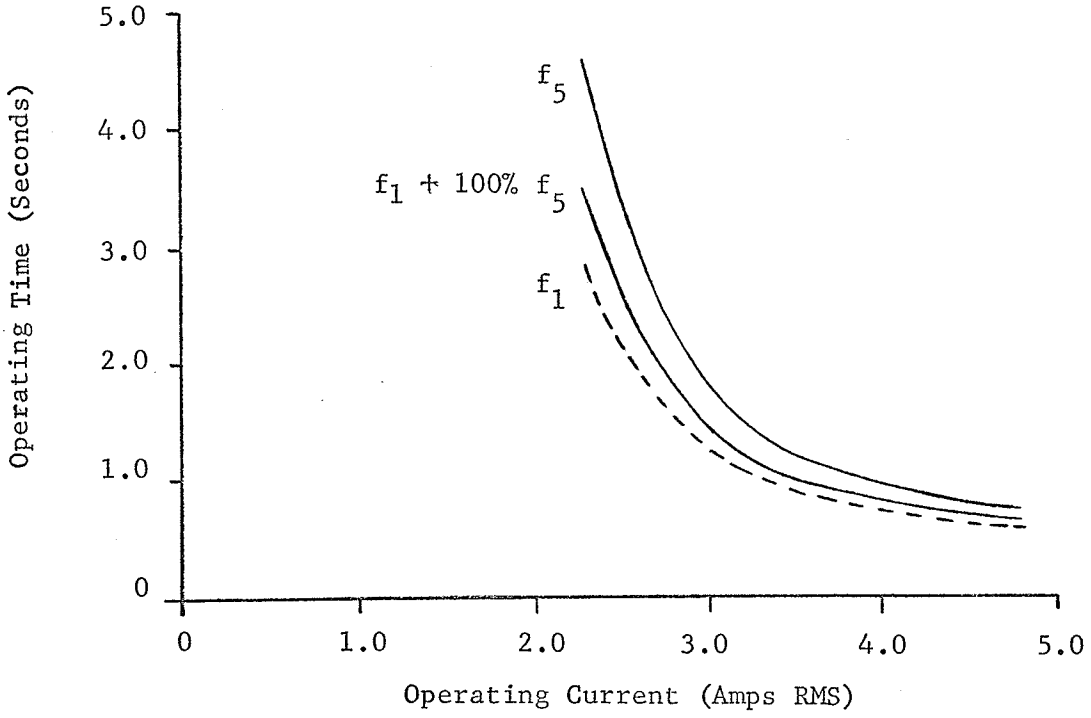

Figure 8a: IAC53 time characteristics with 5th harmonic distortion.

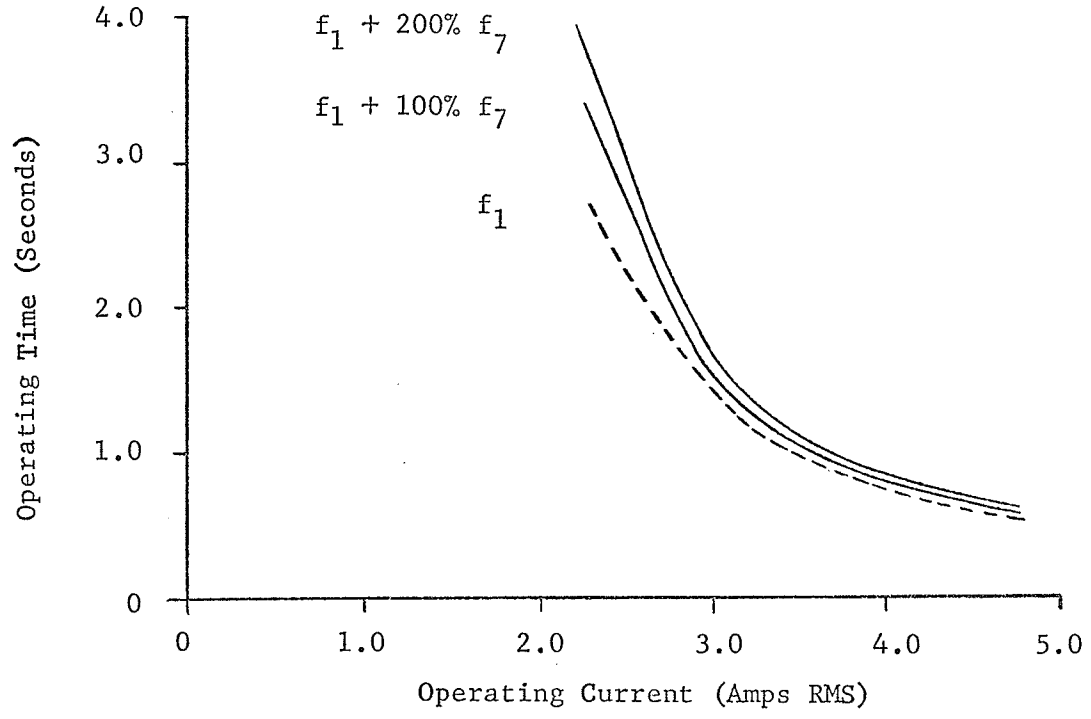

Figure 8b: IAC53 time characteristics with 7th harmonic distortion.

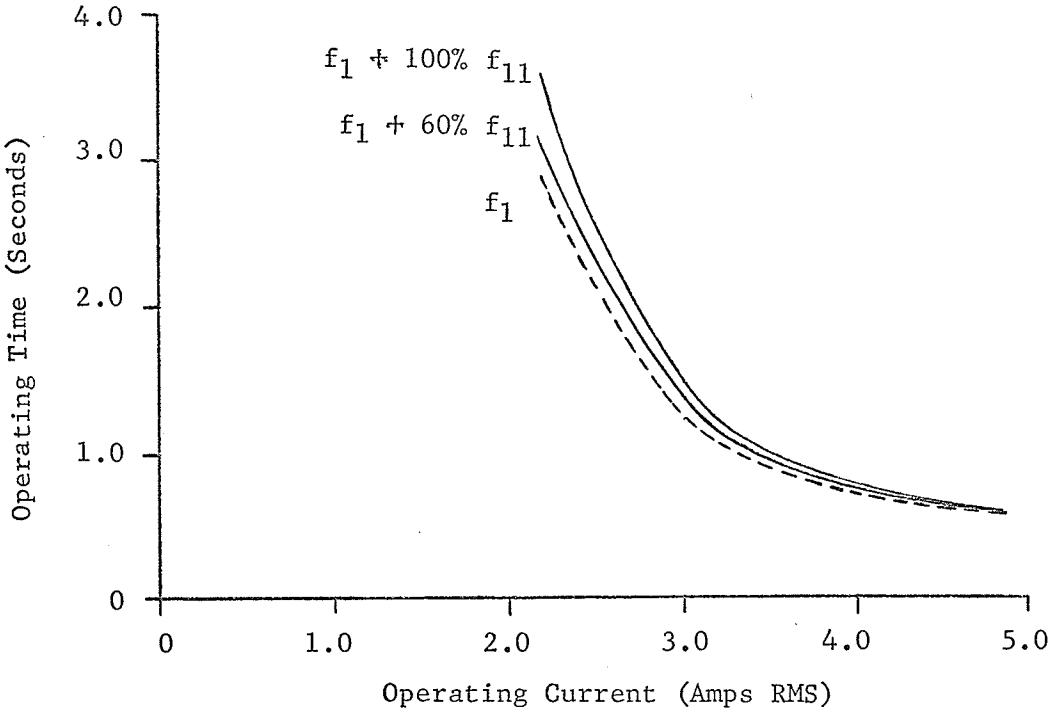

Figure 8c: IAC53 time characteristics with 11th harmonic distortion.

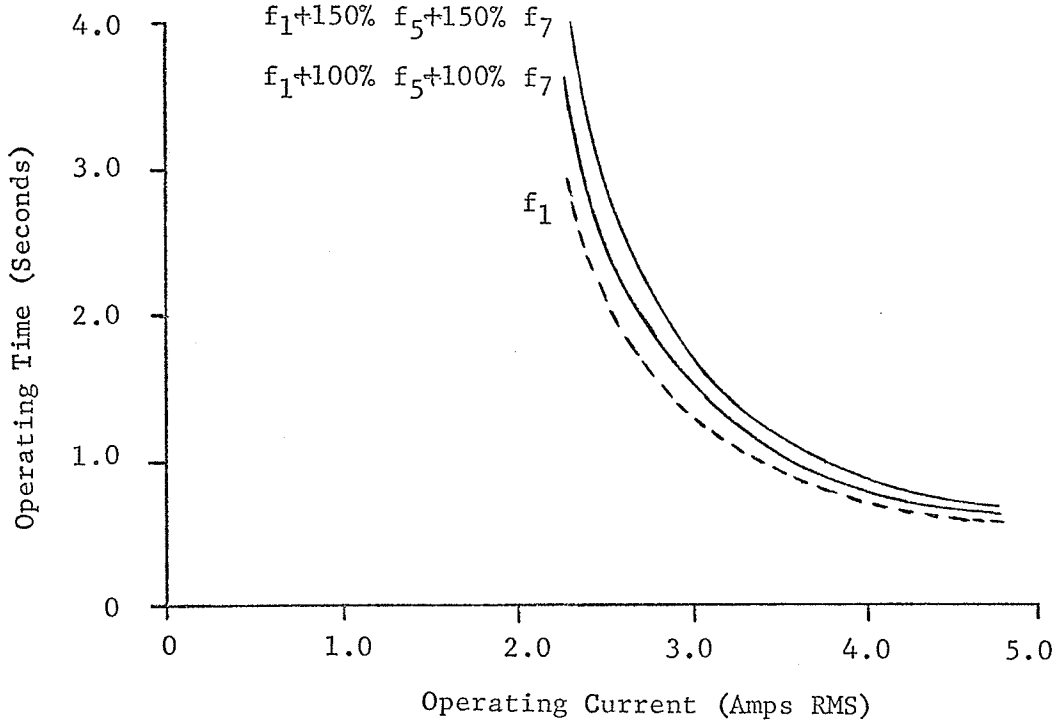

Figure 8d: IAC53 time characteristics with 5th and 7th harmonic distortion.

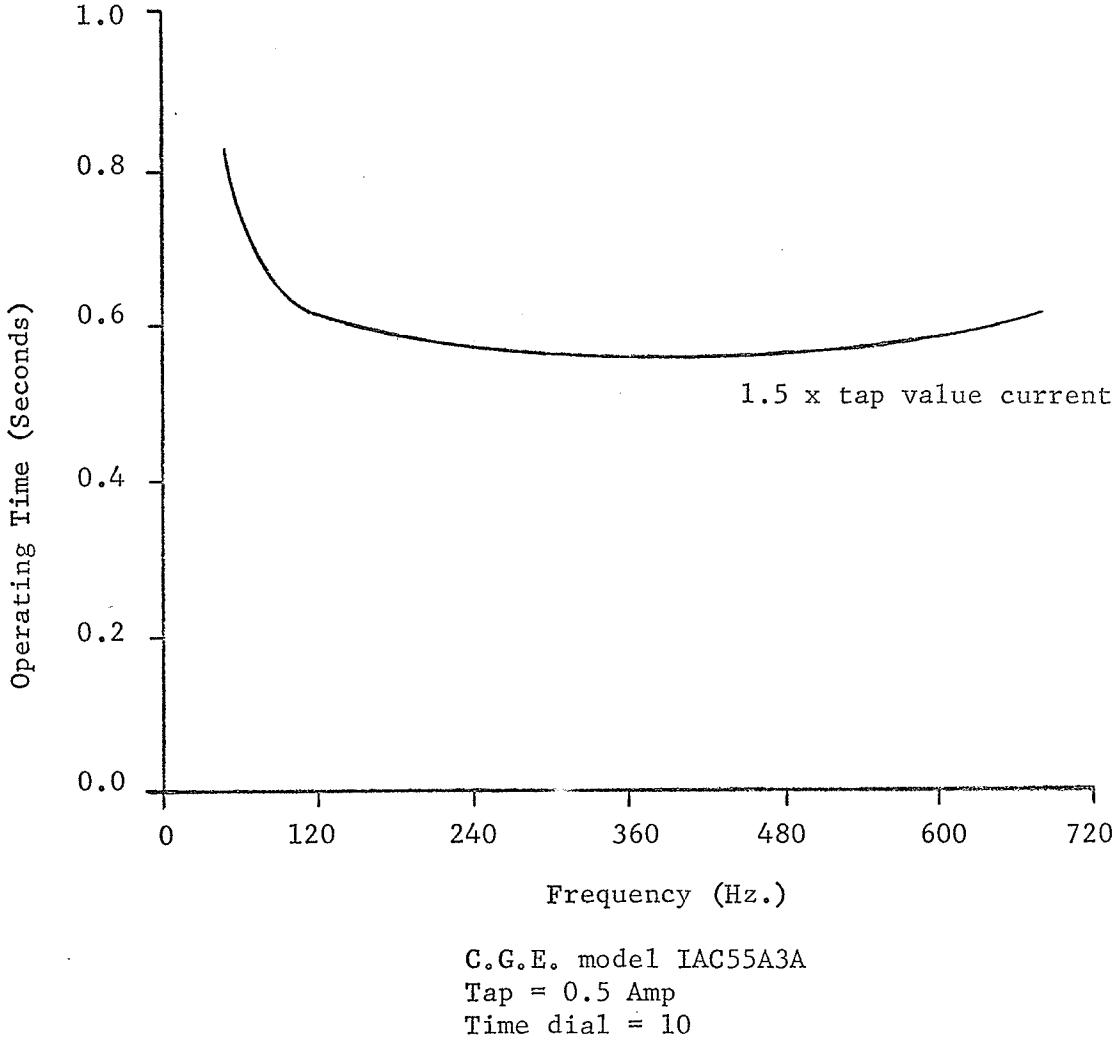

Figure 9: IAC55 frequency response characteristics.

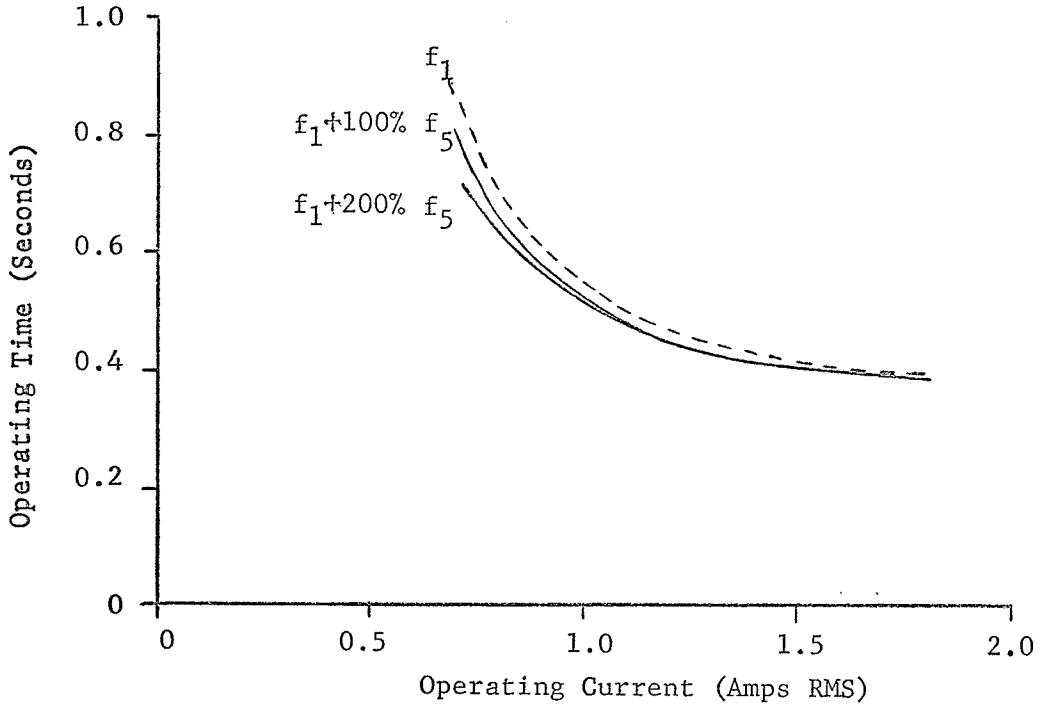

Figure 10a: IAC55 time characteristics with 5th harmonic distortion.

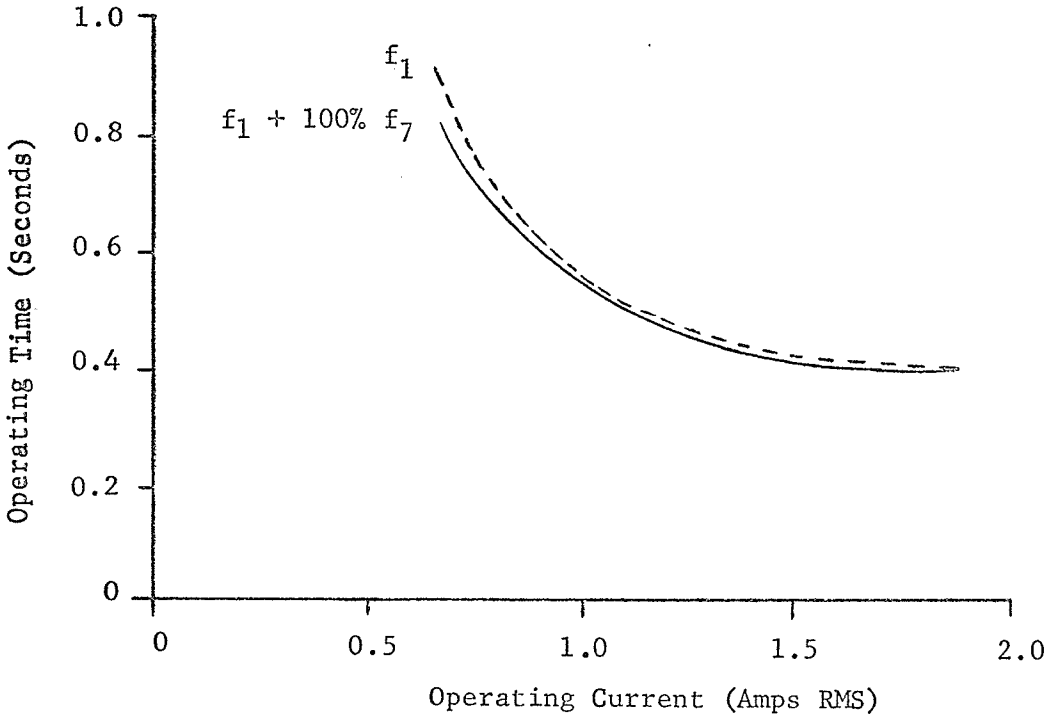

Figure 10b: IAC55 time characteristics with 7th harmonic distortion.

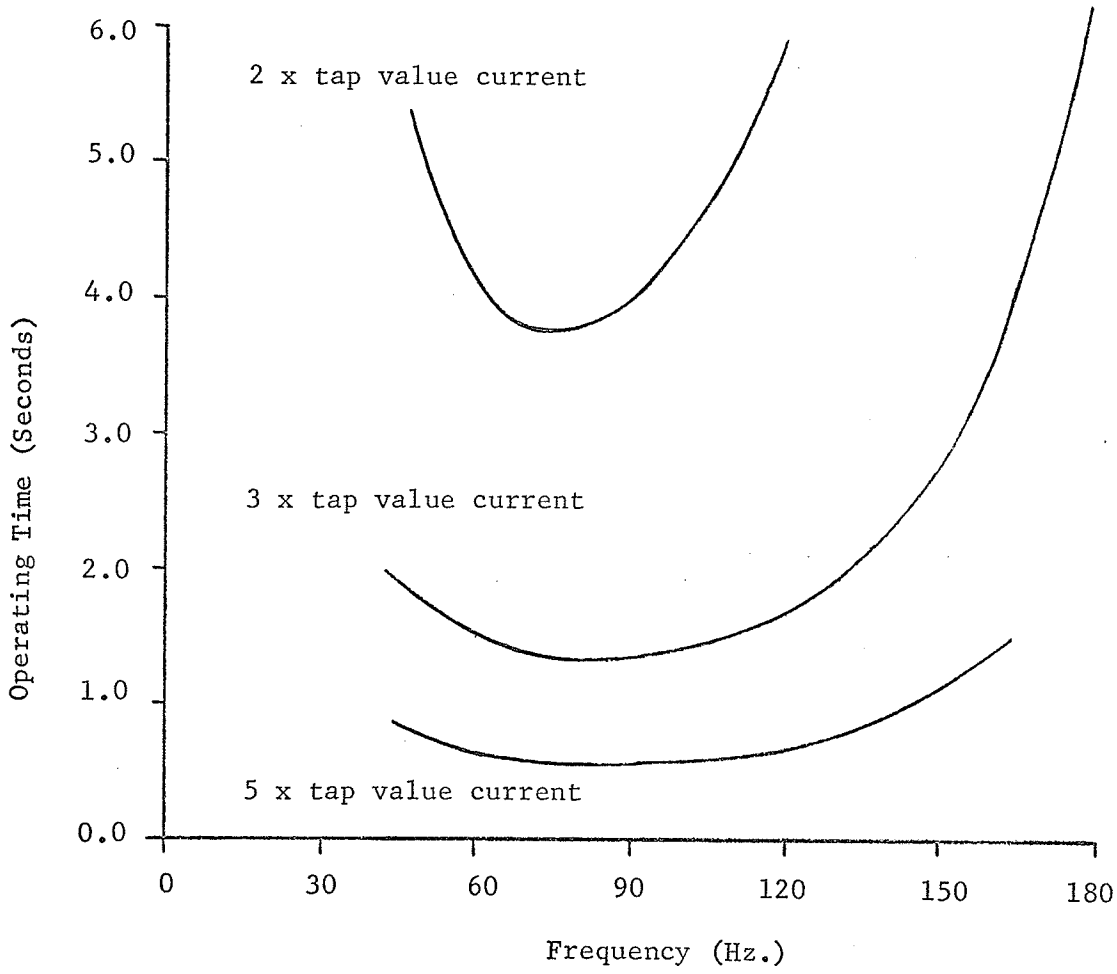

C.W.Co. type CO-8
Style 1875265
Tap = 1 Amp
Time dial = 2

Figure 11: CO-8 frequency response characteristics.

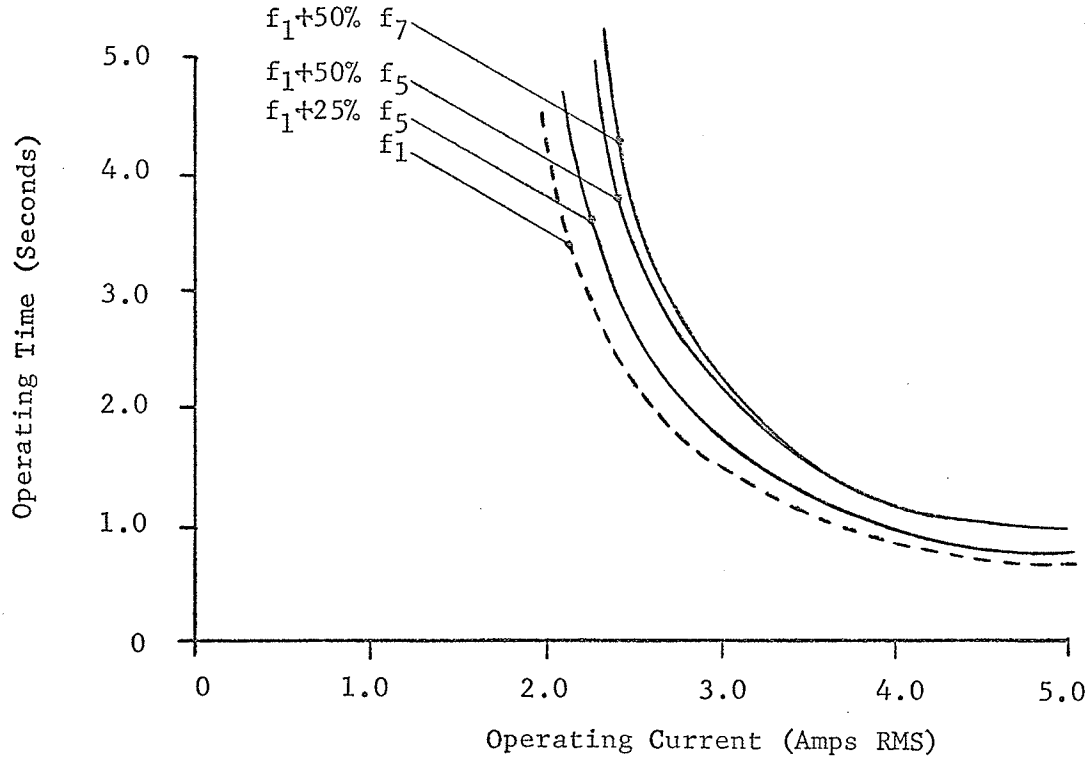

Figure 12a: CO-8 time characteristics with 5th, 7th harmonic distortion.

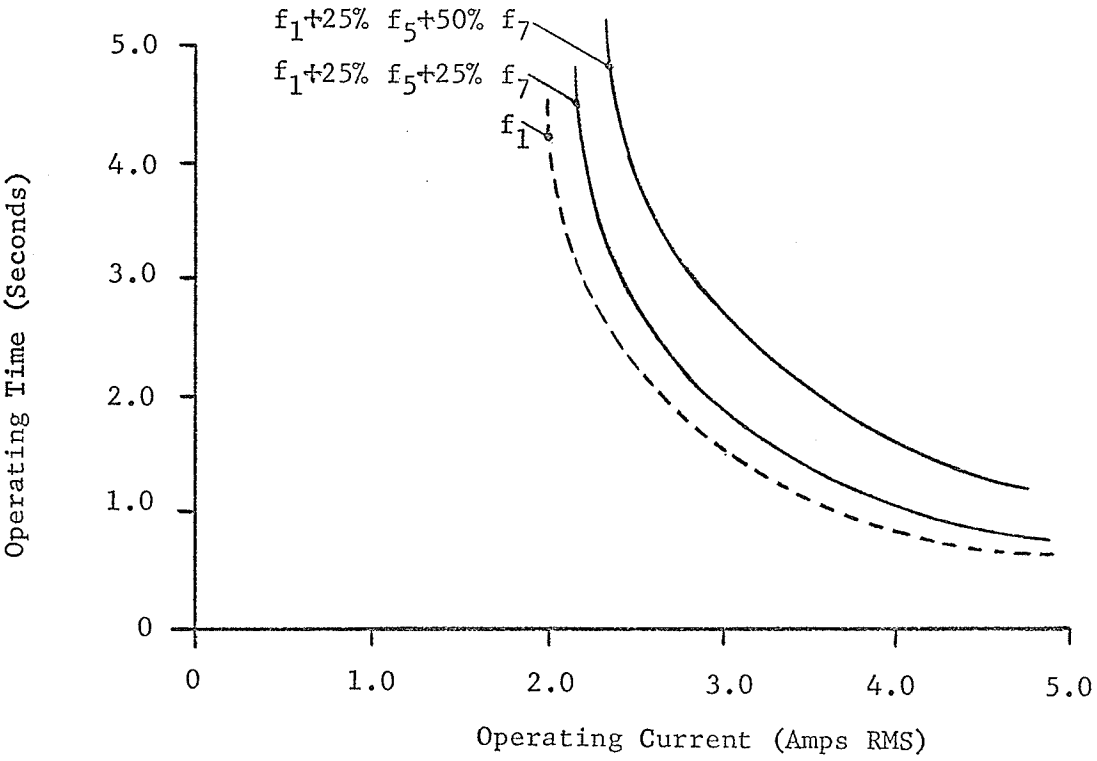

Figure 12b: CO-8 time characteristics with 5th and 7th harmonic distortion.

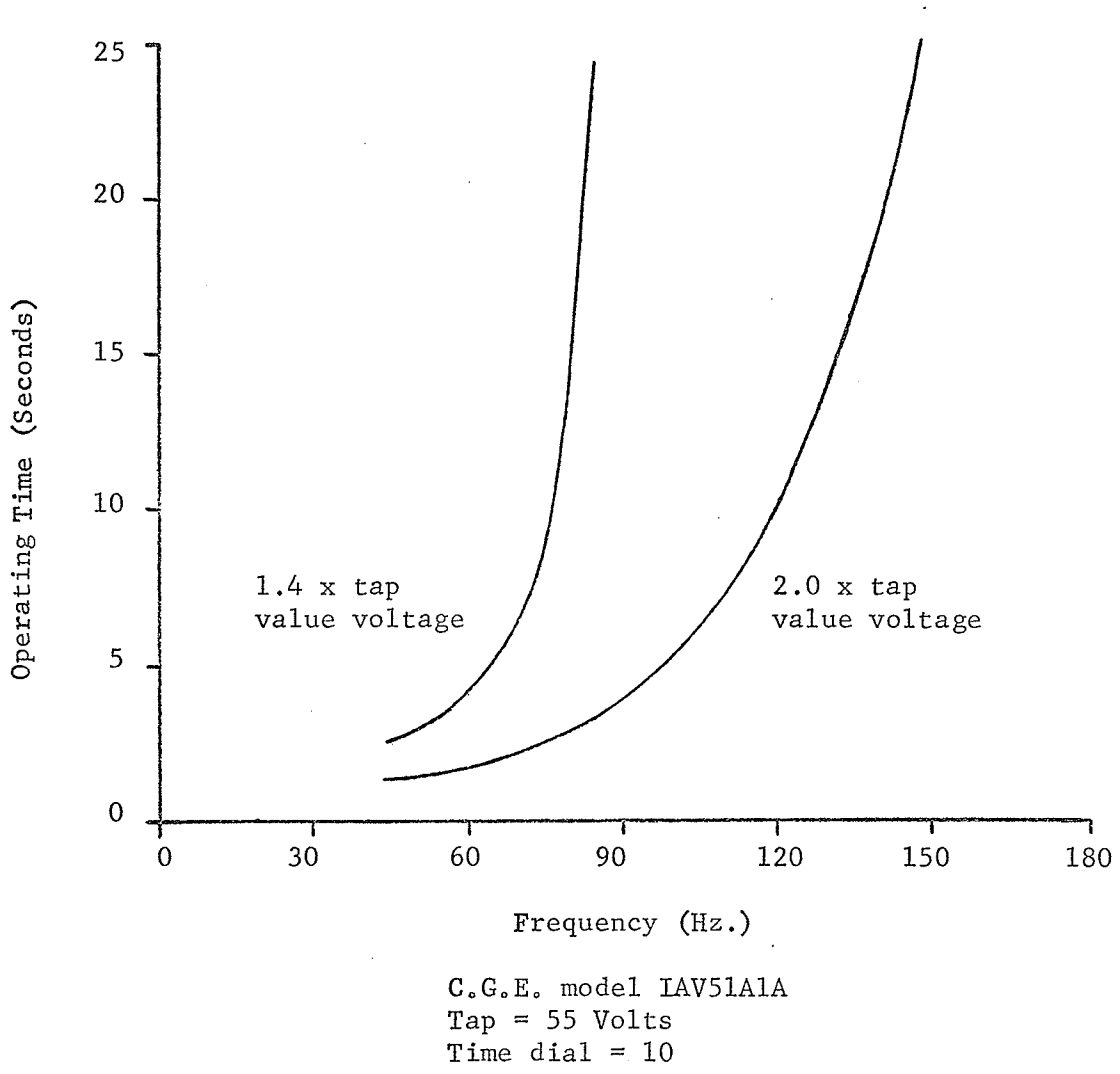

Figure 13: IAV51 frequency response characteristics.

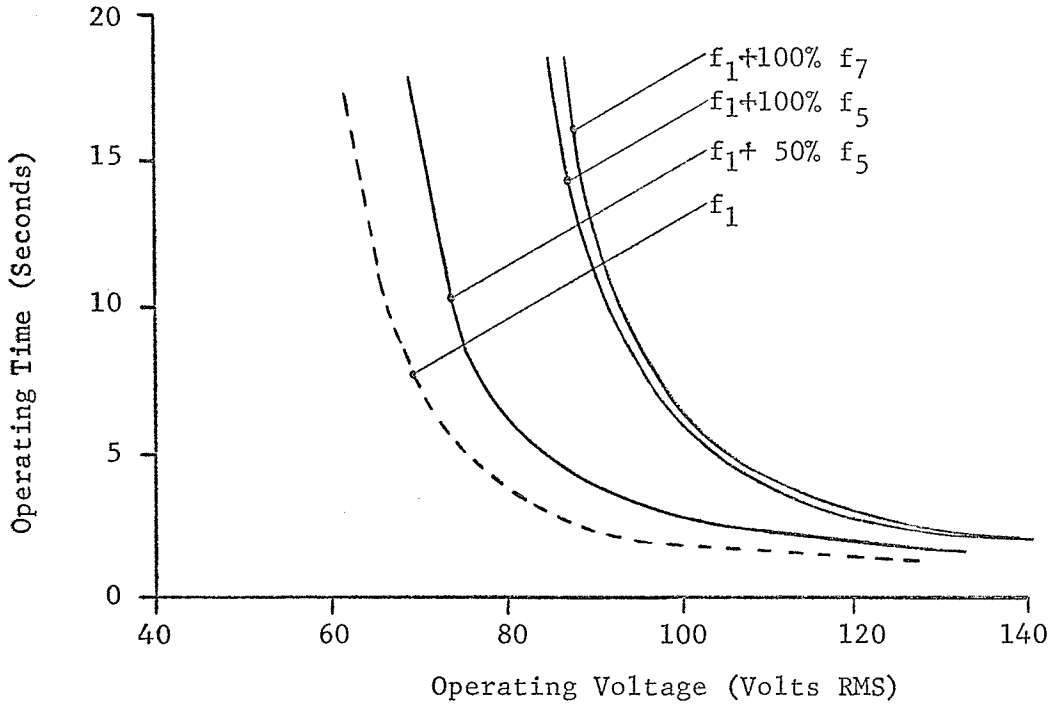

Figure 14a: IAV51 time characteristics with 5th, 7th harmonic distortion.

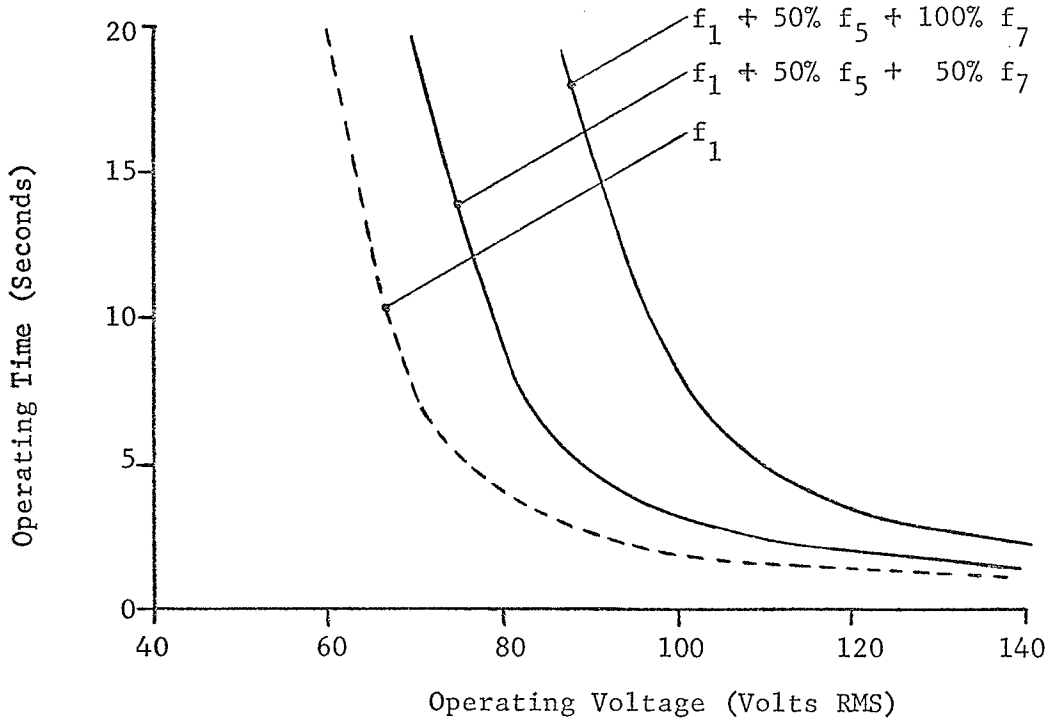

Figure 14b: IAV51 time characteristics with 5th and 7th harmonic distortion.

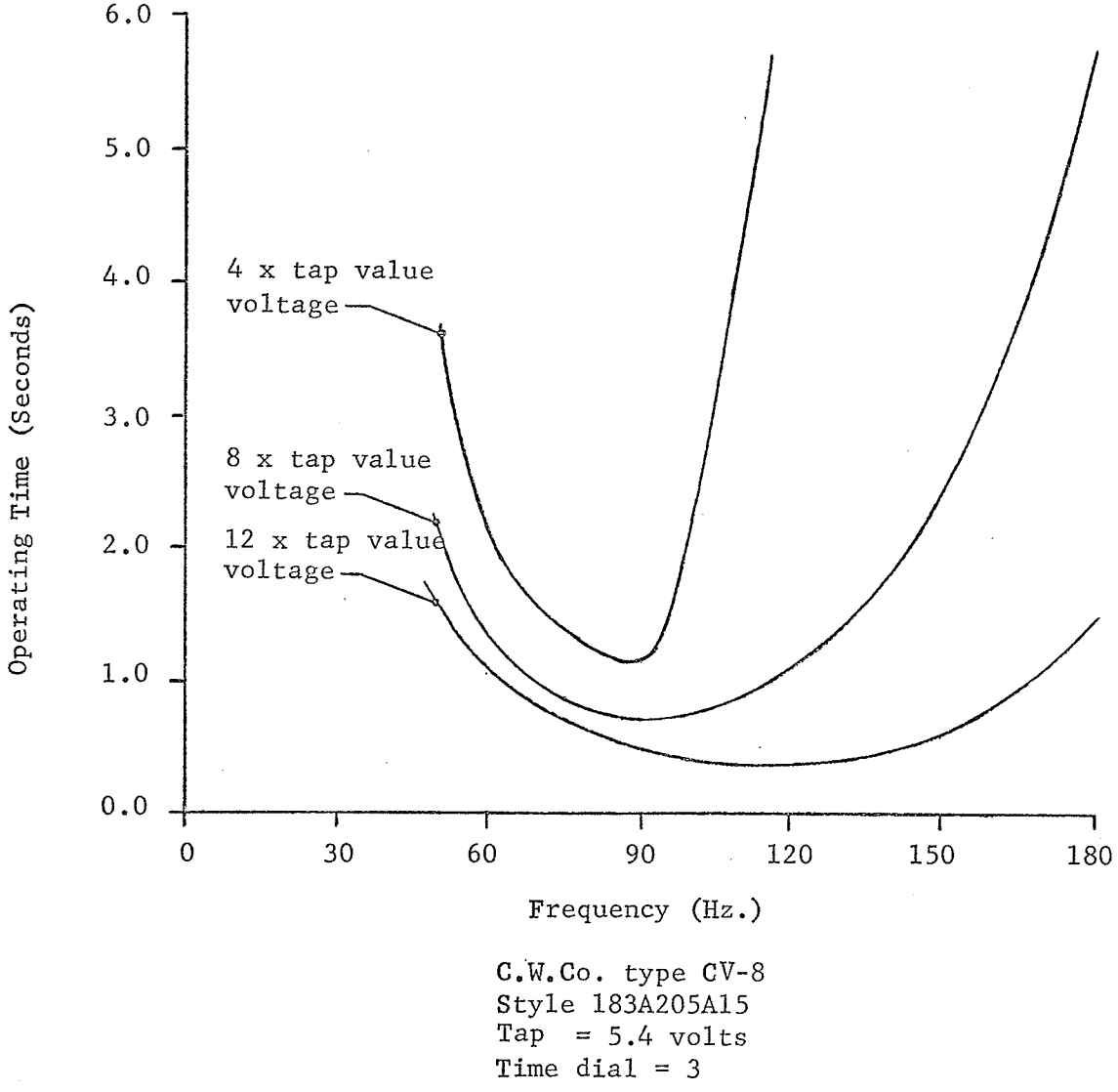

Figure 15: CV-8 frequency response characteristics.

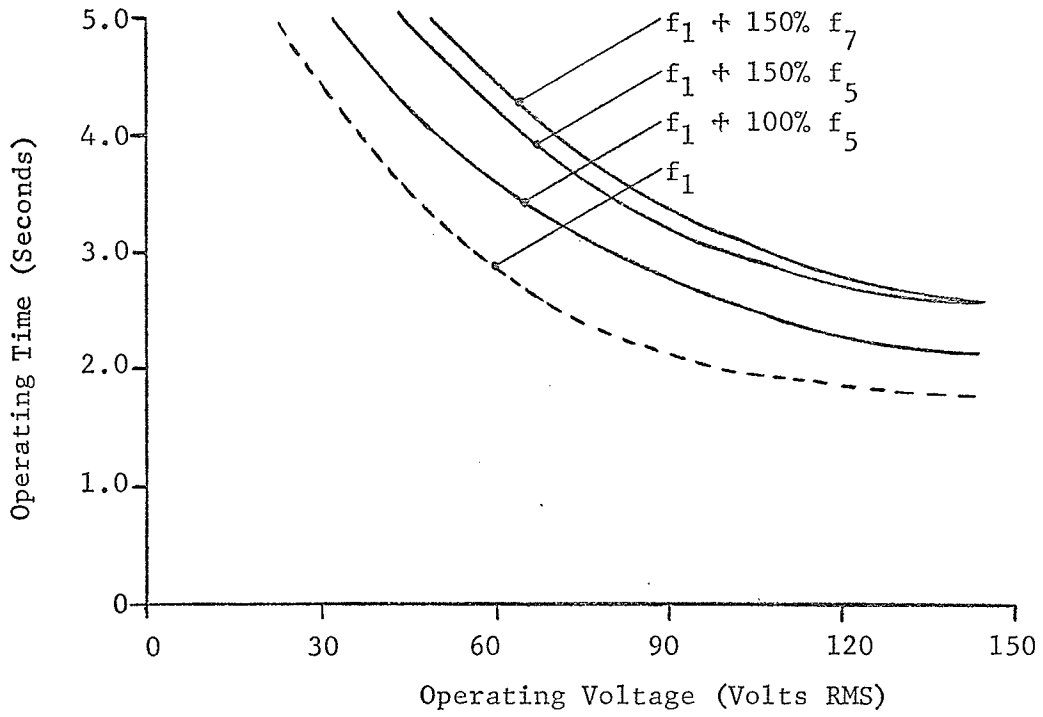

Figure 16a: CV-8 time characteristics with 5th, 7th harmonic distortion.

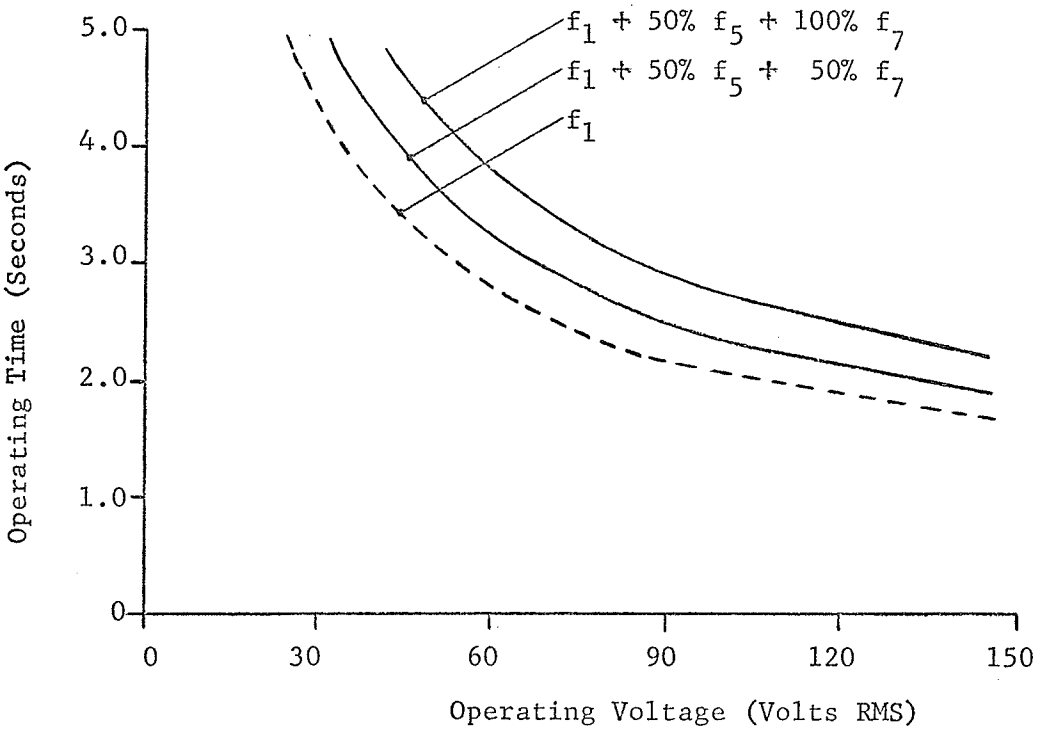

Figure 16b: CV-8 time characteristics with 5th and 7th harmonic distortion.

frequencies. Adding even moderate amounts of harmonics (25 to 50 percent) produced a notable change in characteristics, particularly at low operating current values, with the relay operating slower. This relay also became overheated when subjected to fifth harmonic currents equal to the continuous current rating.

3.3.4 IAV51 - Inverse Time Overvoltage Relay

From figures 13, 14a, 14b it is seen that the operating time for this relay increased with frequency above 50 Hz and rose very sharply above 65 Hz. Adding moderate amounts of harmonics produced a notable change in characteristics at low values of overvoltage with the relay operating slower.

3.3.5 CV-8 - Low Pickup Inverse Time Overvoltage Relay

From figures 15, 16a, 16b it is seen that operating time decreased considerably with frequency above 50 Hz displaying a minimum at 100 Hz. Sharply increased operating times with increasing frequency above this minimum were expected since the relay is designed with a tuned circuit offering a low impedance to fundamental currents and a high impedance to third harmonic currents. Substantial amount of harmonics (100 to 200 percent) were required to produce a major change in characteristics with the relay operating slower.

CHAPTER 4

THEORETICAL ANALYSIS OF TORQUE PRODUCTION IN INDUCTION-TYPE RELAYS

4.1 Effects of Frequency Changes

The results of the tests conducted indicate that obvious changes occur in the time characteristics of certain induction-type relays when varying degrees of harmonic distortion are superimposed on the primary wave form. Certain of the relays operated only slightly slower with impressed harmonics while the CO-8 and IAV51 in particular were very sensitive to harmonic distortion. The CO-8 demonstrated reverse torques at frequencies above 180 Hz. The IAC55 on the other hand actually operated more quickly at low levels of operating current. In all cases the shift in time characteristic was closely related to the frequency response characteristics of the relay.

In order to establish the theoretical relations which are responsible for these effects, it is necessary to explore the physical nature of torque production within these relays.

4.2 Method of Disk Currents

The type IAC53, IAC55 and IAV51 relays tested have a C-shaped magnet structure as shown in Figure 17. In this design the actuating flux which pierces the aluminum disk is split into two out-of-phase components by copper shading rings that encircle part of the pole face of each pole at the air gap. The flux distribution at fundamental frequency is approximately as shown in Figure 18[8]. Figure 19 indicates how force is developed in the moveable disk by interaction of the electromagnetic fluxes with eddy currents that are induced in the disk by these

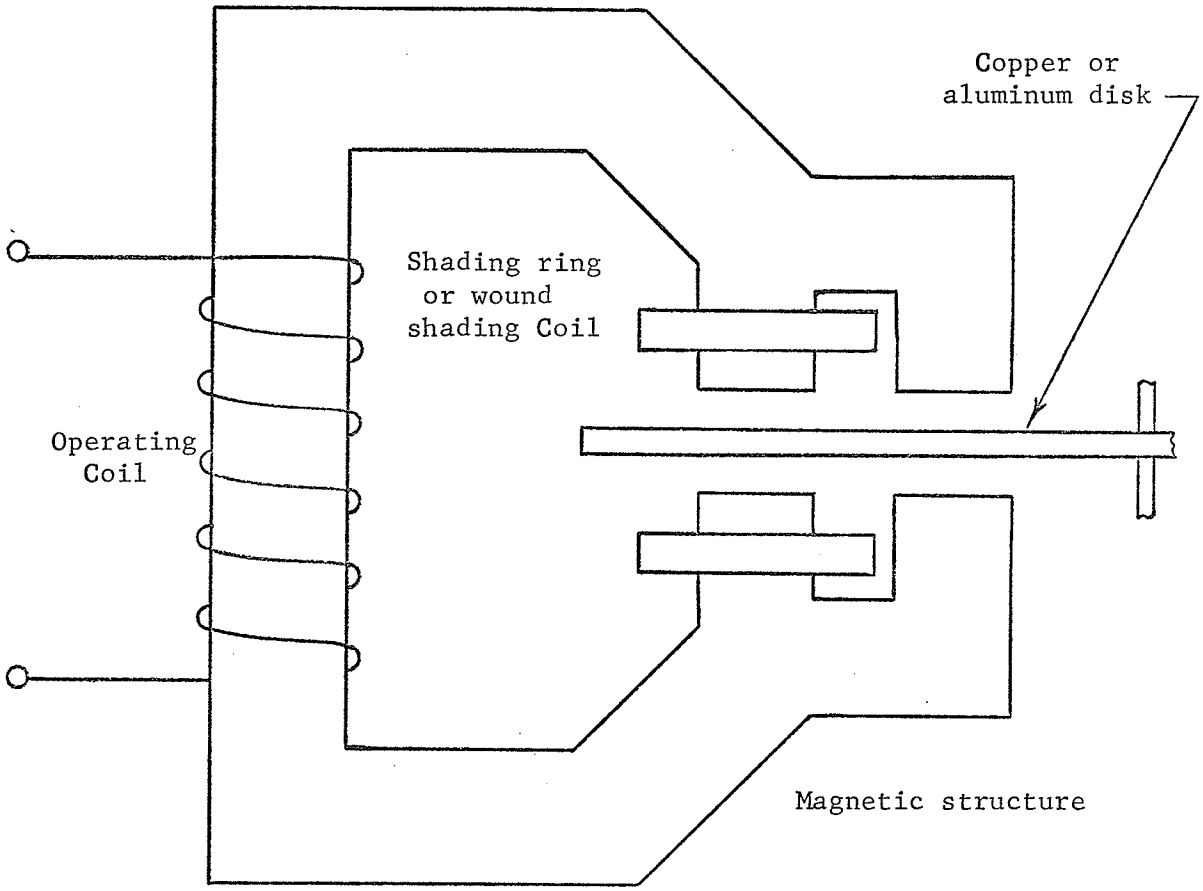

Figure 17: C-shaped electromagnet structure.

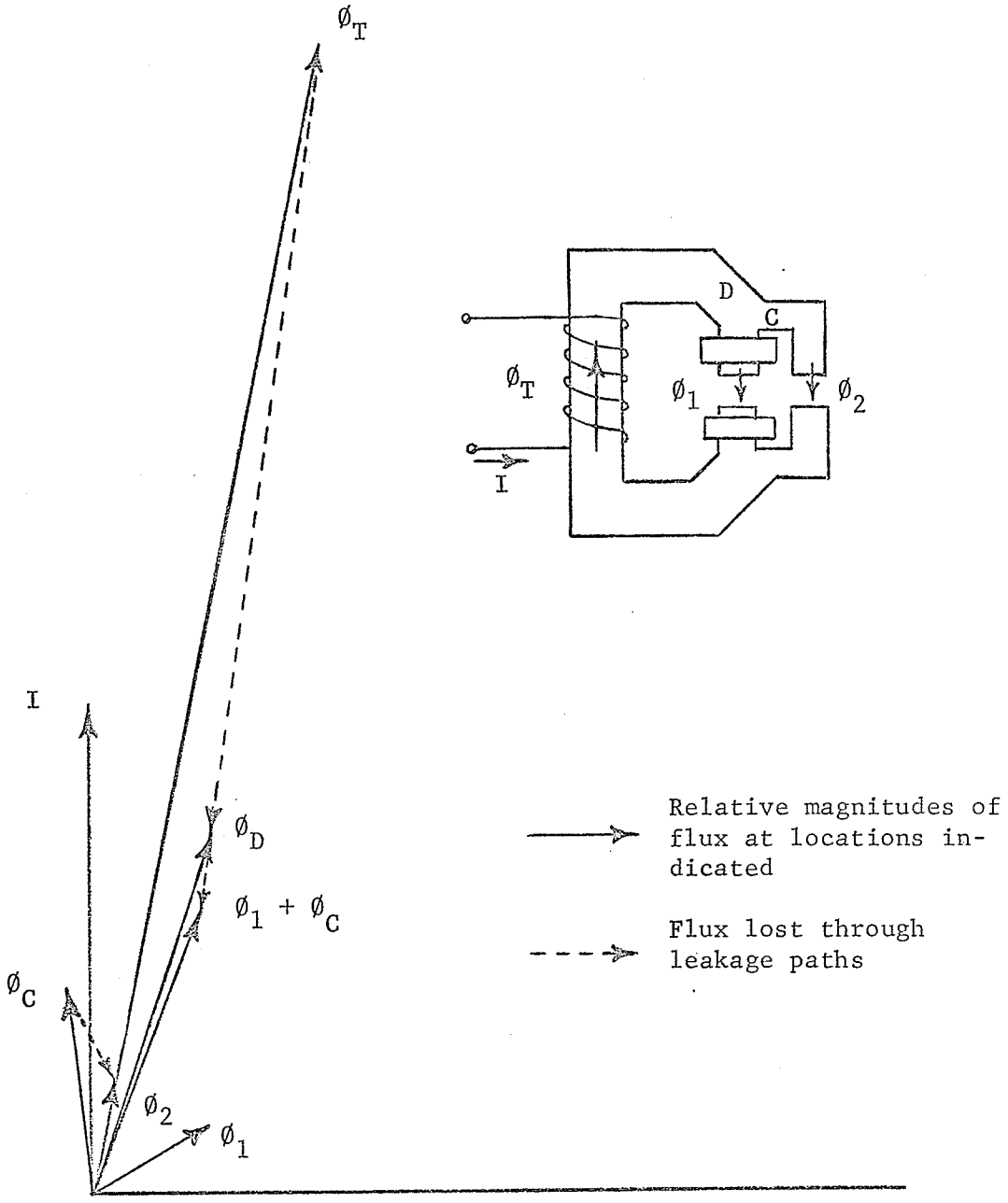

Figure 18: Flux distribution in C-shaped electromagnet at rated frequency.

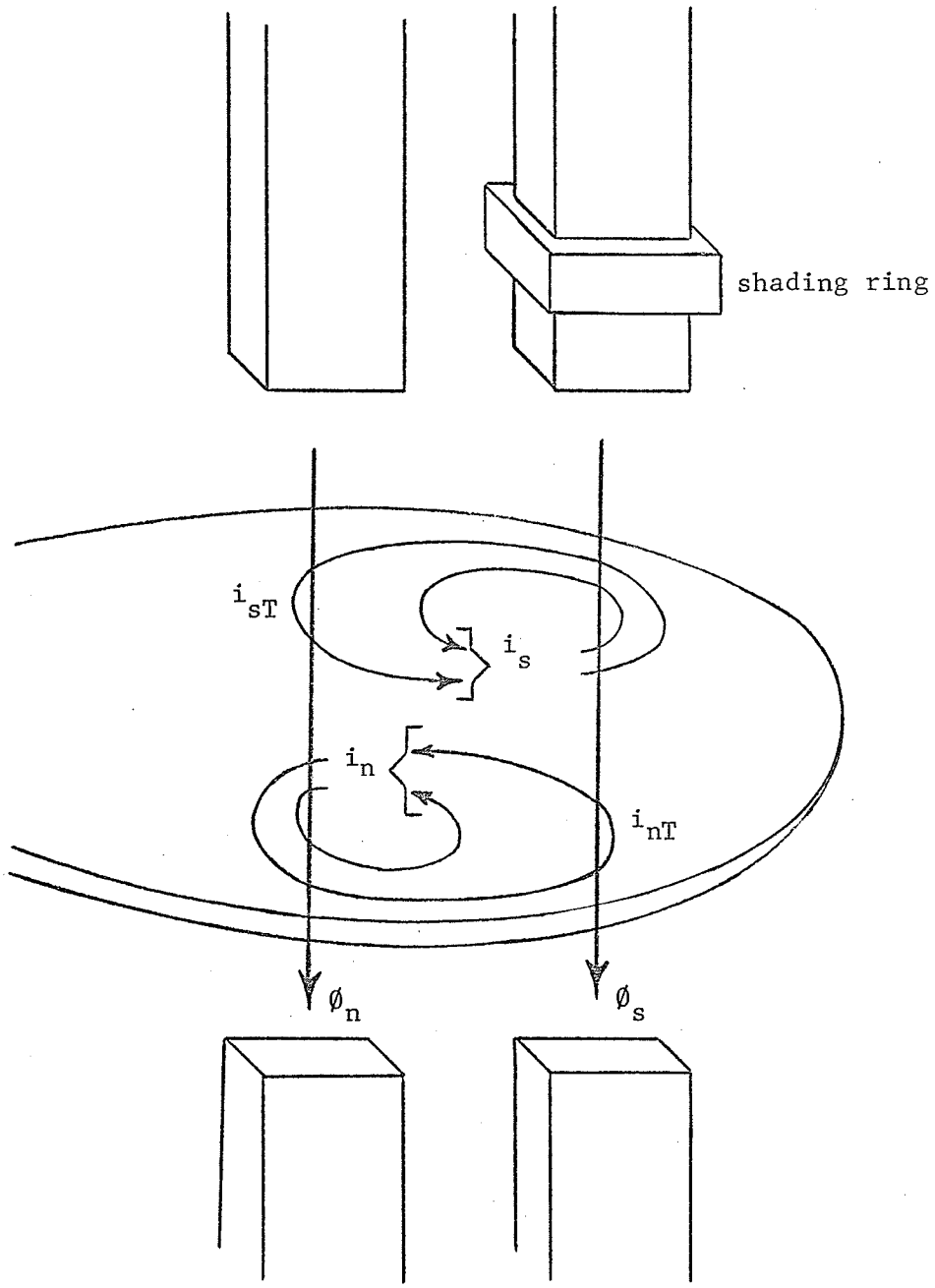

Figure 19: Development of torque in an induction disk relay.

fluxes.

If ϕ_n and ϕ_s are the two alternating magnet fluxes, in unshaded and shaded poles respectively, passing through the disk their normal components within the disk may be given by:

$$\phi_n = K_a \; I_n \; \sin (wt + \alpha_n)$$

$$\phi_s = K_a \; I_s \; \sin (wt + \alpha_s)$$

where I_n and I_s are the amplitudes of the input currents developing the respective fluxes and K_a represents the magnetic circuit constants. If the effective impedances presented by the disk to currents induced by the two fluxes is equal and given as $Z \angle \lambda$, then the total currents in the disk become:

$$i_n = - \frac{d\phi_n/dt}{Z \angle \lambda} = - \frac{wK_a \; I_n}{Z} \cos (wt + \alpha_n - \lambda)$$

$$i_s = - \frac{d\phi_s/dt}{Z \angle \lambda} = - \frac{wK_a \; I_s}{Z} \cos (wt + \alpha_s - \lambda)$$

The portions of these induced disk currents which react with the resultant flux of the other pole, thereby producing torque may be defined as:

$$i_{nT} = K_b \; i_n$$

$$i_{sT} = K_b \; i_s$$

Where K_b is another constant which can be assumed equal for both currents such that:

$$K_b = \frac{i_{nT}}{i_n} = \frac{i_{sT}}{i_s}$$

By assuming that the paths in which the disk currents flow

have negligible self-inductance the shading effect of the disk, or effect of the induced currents upon the applied fluxes, may be neglected. Torque is produced by the interaction of each flux with the appropriate portion of the disk current induced by the other flux:

$$T = K_c \quad (i_{nT} \quad \phi_s \quad - i_{sT} \quad \phi_n)$$

Substituting the appropriate values of fluxes and disk currents from above into this equation yields:

$$T = \frac{wK_a^2 \quad K_b \quad K_c}{Z} \quad I_n \, I_s \quad \sin \, (\alpha_n \quad - \alpha_s) \quad \cos \lambda$$

Using rms quantities and considering $I_1 = I_2$ for a single quantity relay:

$$T = KwI^2 \quad \sin \quad \theta \quad \cos \lambda$$

where $K = \frac{2K_a^2 \, K_b \, K_c}{2}$

θ = phase shift between fluxes $(\alpha_n - \alpha_s)$

This form of the torque expression is in agreement with the accepted form of the universal relay-torque equation[4] which expresses, neglecting the effect of saturation, the net torque of all single quantity induction relays in the form:

$$T = K_1 \quad I^2 \quad - \quad K_2 \qquad \text{or} \qquad K_1 \, V^2 \quad - \quad K_2$$

where I and V are the rms magnitudes of the total current or voltage respectively of the two circuits and K_1 and K_2 are appropriate constants.

It is seen that the phase angle relationship between the individual operating quantities may be taken as a design constant and does not enter into the application of these relays. However, the effects of changes in w and changes in phase angle λ of the disk impedance must be considered if frequency variations are to be allowed to occur. In the

developed relationship torque is related in direct proportion to frequency. Evidence of this effect was seen to occur in most of the relays tested where operating speeds increased with increasing frequency below 60 Hz and for a narrow region above 60 Hz. At higher frequencies however, the operating times increased or at best remained constant.

4.3 Method of Shifting Disk Fluxes

The type CO-8 and CV-8 relays tested have an E-shaped magnet structure as shown in Figure 20. Although the previous calculation of disk torques from disk currents is equally adaptable to this structure, a different approach in terms of shifting disk fluxes provides some particularly worthwhile insights. The manner in which the electromagnet furnishes a shifting flux to produce torque can be seen be developing a transformer type vector diagram as shown in Figure 21[12]. Only the components of flux actually crossing the air gap are considered while the various other leakage fluxes are ignored.

With proper reference directions the vector diagram can be rearranged to show the correct relative phase angles for predicting relay operation. This is done in Figure 22. The fluxes are seen to be out of phase with each other and arranged in such a manner that a shifting 3-phase field is involved. This set of vectors may then be analyzed by breaking it down into positive, negative and zero sequence symmetrical components of the three fluxes. Changing the relative proportions, both magnitudes and phase angles, will make changes in the way these three vectors break down into their sequence components.

Applying the symmetrical component analysis to the fluxes involved, the torque produced by the electromagnet may be considered in terms of the following components[12]:

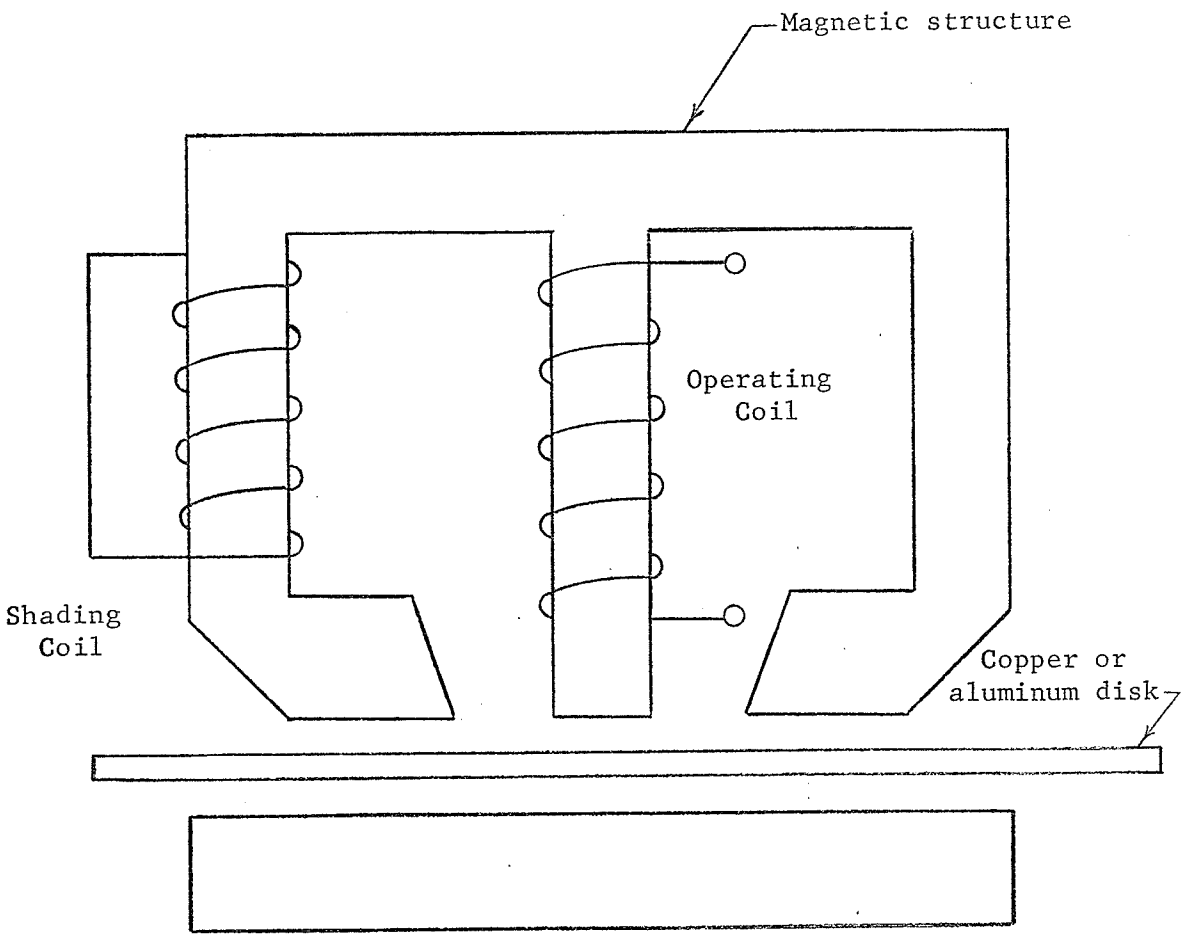

Figure 20: E-shaped electromagnet structure.

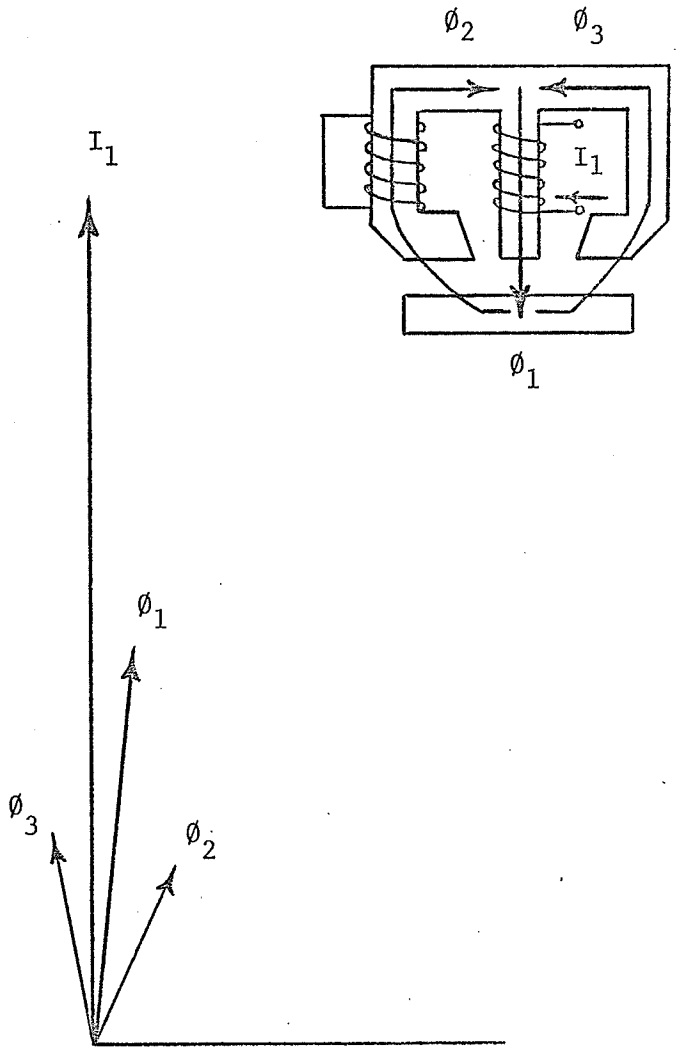

Figure 21: Flux distribution in E-shaped electromagnet at rated frequency.

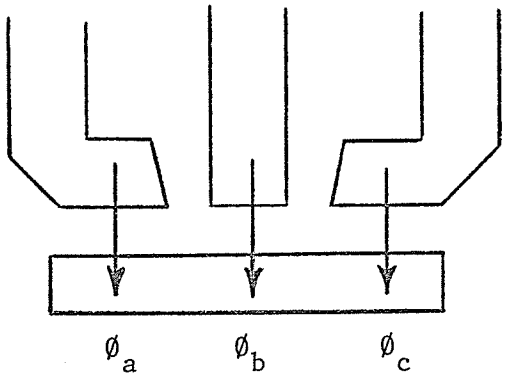

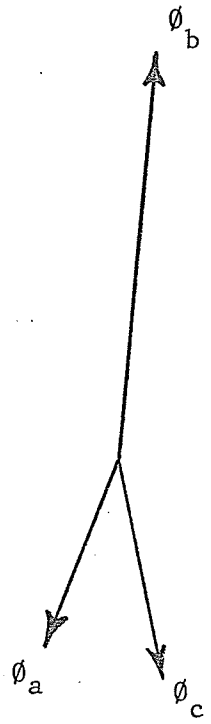

Figure 22: Vector diagram of air gap fluxes.

$$T_1 = T_2 + T_{sd} + T_d + T_s$$

The first three terms defining torques produced by the electromagnet may be expressed as a function of the electromagnet flux:

$T_1 = K\phi_1^2$ = the positive sequence component of torque.

$T_2 = K\phi_2^2$ = the negative sequence component of torque.

$T_{sd} = P\phi_1^2 (1 + \phi_2^2/\phi_1^2)S = P\phi_1^2 (1 + b^2)S$ = a self-damping torque produced by the ac fluxes of the electromagnet.

Where K = a constant of the magnetic circuit

ϕ_1, ϕ_2 = positive and negative sequence fluxes

P = a constant pertaining to self-damping

b = the ratio ϕ_2/ϕ_1

S = the speed of the disk

The last two terms of the torque expression are design constraints of the relay:

$T_d = K_d S$ = torque produced by damping magnet

$T_s = G$ = torque exerted by restraint spring

In terms of these definitions the expanded torque equation becomes:

$$K\phi_1^2 = K\phi_2^2 + P\phi_1^2 (1 + b^2)S + K_d S + G$$

Considering a given disk driven by positive sequence torque only with factors $K_d = G = b = 0$ so that their effects are suppressed, the speed, S_1, of the disk can be given as:

$$S_1 = \frac{K\ \phi_1^2}{P\ \phi_1^2} = \frac{K}{P}$$

The term K/P is the "synchronous" or maximum speed of the disk assembly when energized with positive sequence torque only. It will remain unchanged unless the frequency or the pole configuration of the electromagnet is changed.

Likewise, by letting $K_d = G = 0$ so that their effect in the extended torque equation is suppressed, a similar expression for the speed S_o of the free-running disk driven by the actual electromagnet may be developed:

$$S_o = \frac{K\,(\phi_1^2 - \phi_2^2)}{P\,\phi_1^2\,(1 + b^2)} = \frac{K\,\phi_1^2\,(1 - b^2)}{P\,\phi_1^2\,(1 + b^2)}$$

from which

$$b = \sqrt{\frac{1/S_o - P/K}{1/S_o + P/K}}$$

The term b may be a constant or variable depending on whether or not the ratios $1/S_o$ and P/K remain constant throughout the operating range.

From the above the constant P will remain unchanged for fixed frequency and pole configuration. Speed of the disk is then directly a function of $b = \phi_2/\phi_1$. This effect forms the basis for controlling operating characteristics by adjusting the relative magnitudes of the positive and negative sequence components of flux passing through the disk, acting somewhat as an efficiency factor for the electromagnet. The CO-8 relay tested was observed to have two adjustable magnetic plugs in the core structure for exactly this purpose, the changing efficiency overshadowing the effect of the plugs on saturation at higher currents.

Considering further the effect of increasing frequency on the overall torque characteristics:

From $S_1 = \frac{K}{P}$, operating time which is proportional to $\frac{1}{S_1}$ decreases with frequency since $\frac{K}{P}$ can be taken as increasing in direct proportion to frequency.

From $S_o = \frac{K\ (1 - b^2)}{P\ (1 + b^2)}$, operating time which is proportional to $\frac{1}{S_o}$ becomes dependent on any changes occurring in b.

The overall nature of these effects is shown in Figure 23. The cumulative result is seen to be largely dependent on the nature of b. As b approaches 1, the operating torque of the electromagnet will reduce to zero. Also it is quite possible for the magnitude of ϕ_2 to exceed ϕ_1. The direction of the resultant torque of the electromagnet will reverse as shown by the negative sign in the ratio of $(1 + b^2)/(1 - b^2)$, $b > 1$. It will increase in that direction as the ratio $(1 + b^2)/(1 - b^2)$ approaches unity once again in the negative sense.

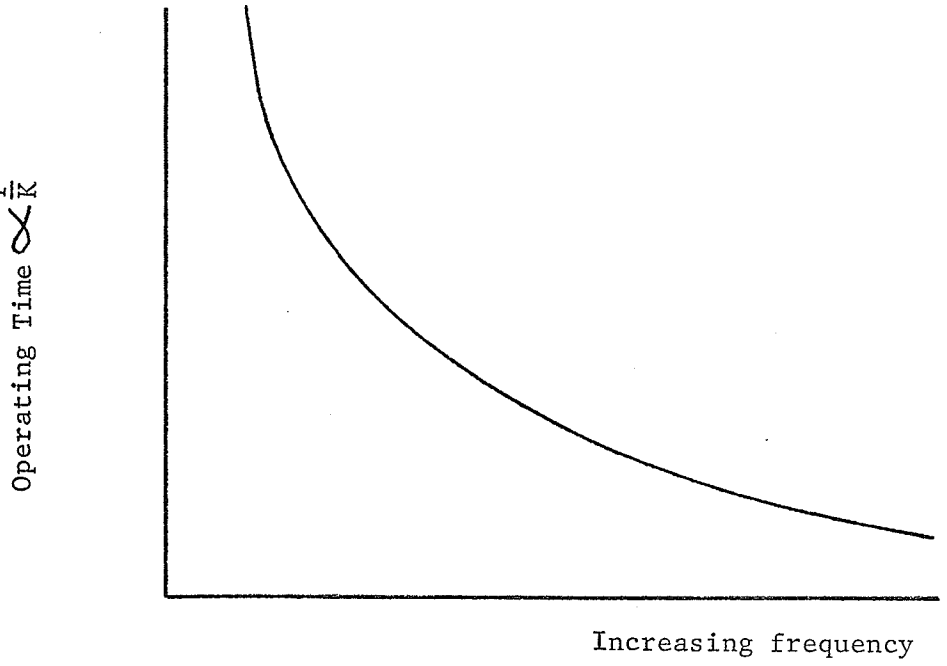

Figure 23a: Proportionality of operating time to frequency.

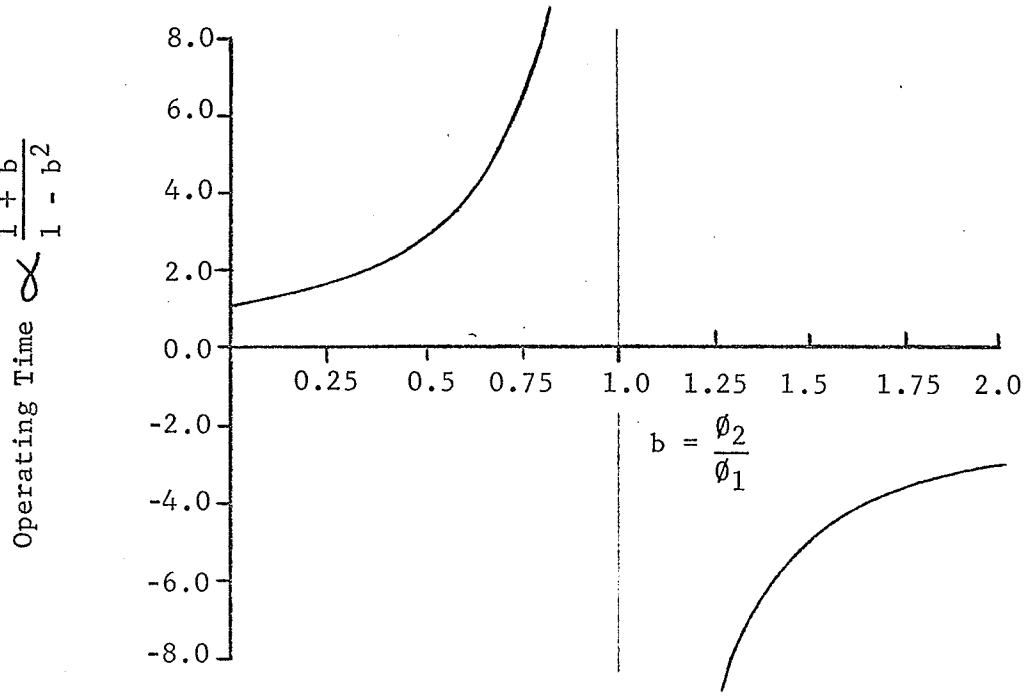

Figure 23b: Proportionality of operating time to ratio of positive and negative sequence fluxes.

CHAPTER 5

FLUX BEHAVIOUR IN INDUCTION RELAY AIR GAPS

5.1 Significance of Air Gap Fluxes

In Section 4.3 it has been developed that the relative proportions between the air gap fluxes and the manner in which they break down into positive, negative and zero sequence components has a direct bearing on the torque relationships within the disk of an induction disk type of relay. Among the various theoretical relations developed for torque production this was the only consideration which encouraged an explanation of the reverse torque developed in the CO-8 relay at higher frequencies. A method of verifying this behaviour was required. It was decided to carry out a survey of air gap flux behaviour under varying frequency conditions.

5.2 Measurement of Air Gap Fluxes

The survey of air gap fluxes was carried out by winding search coils around the appropriate portions of the relay magnetic circuits. For these tests ten turn search coils were used in all cases so that relative magnitudes could be compared. By integrating the voltage induced in the search coils with respect to time, the flux conditions within the coil were directly available as voltages:

$$\phi = \Phi_m \sin wt = \frac{1}{N} \int e \, dt$$

where e = voltage induced in search coil

N = number of turns in search coil

Φ_m = peak value of flux wave

The quantities were integrated by means of an analogue computer so that suitable gains could be introduced to facilitate monitoring on an oscilloscope. A programmable bipolar operational power supply was used as the power amplifier in these tests. The high degree of feedback inherent in this device insured that truly sinusoidal operating quantities were being supplied to the relay under test despite any nonlinearities in relay impedance which may have resulted under the varying frequency conditions.

5.2.1 CO-8 - Very Inverse Time Overcurrent Relay

The CO-8 relay was tested by having search coils wound on each of the three separate legs of the E-shaped magnetic structure. The results are shown in Figures 24a and 24b for frequencies of 70 Hz and 300 Hz respectively. It is seen that the magnitude of the negative sequence component exceeds that of the positive sequence component at 300 Hz. This is in complete agreement with the reversal in direction of torque occurring between these two frequencies.

5.2.2 CDG13 - Very Inverse Time Overcurrent Relay

It was desired to conduct a similar survey of air gap flux conditions in a relay with a C-shape electromagnet such as the IAC53. Unfortunately this relay had a pole face and shading ring structure which did not readily permit winding of the search coils around the pole faces at the air gap. A CDG13 relay was used instead. This relay had almost an identical electromagnet structure and similar published time characteristics as the IAC53[15].

The results of varying frequency on the air gap fluxes of the two poles is shown in Figure 25. It is seen that the phase shift between the two pole face fluxes produced by the electromagnet is re-

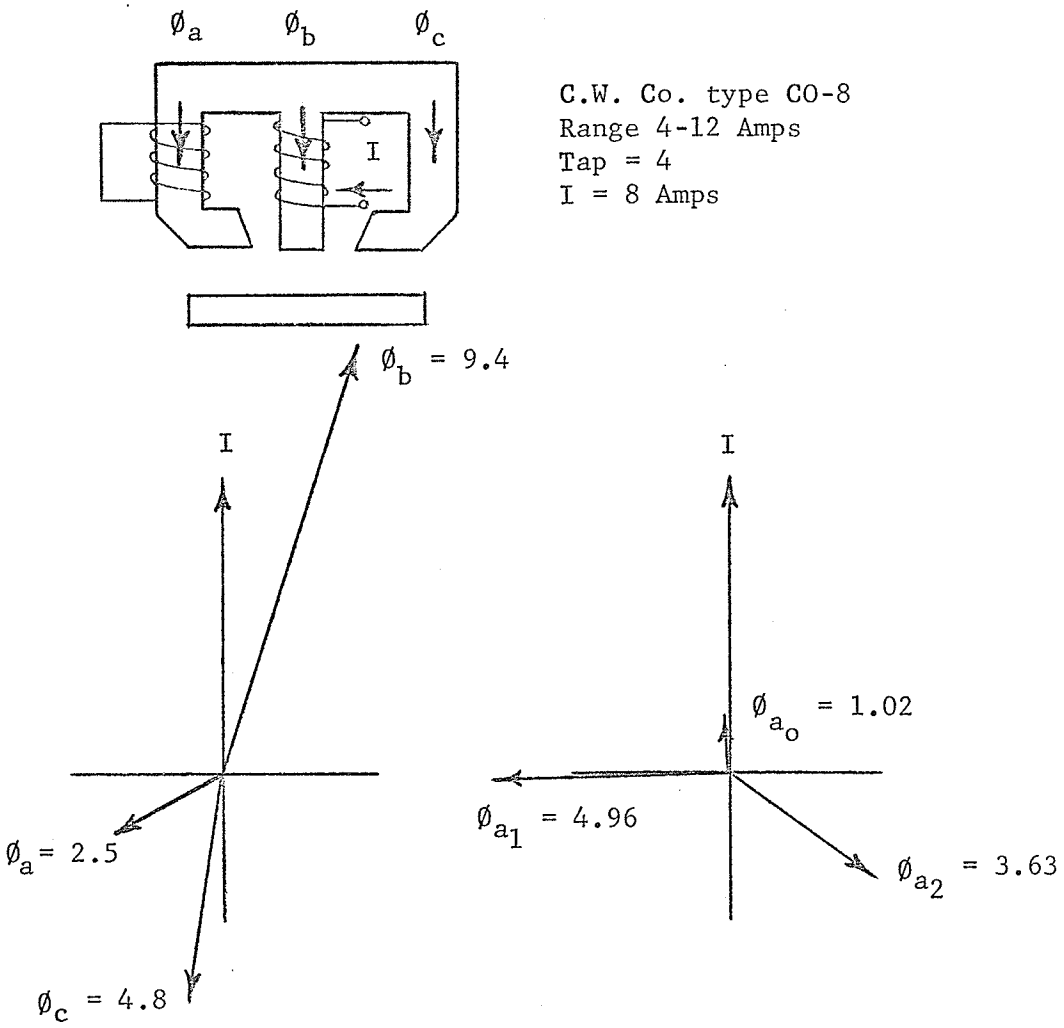

Figure 24a: CO-8 flux distribution at 70 Hz. (Relative magnitudes in 'millivolts').

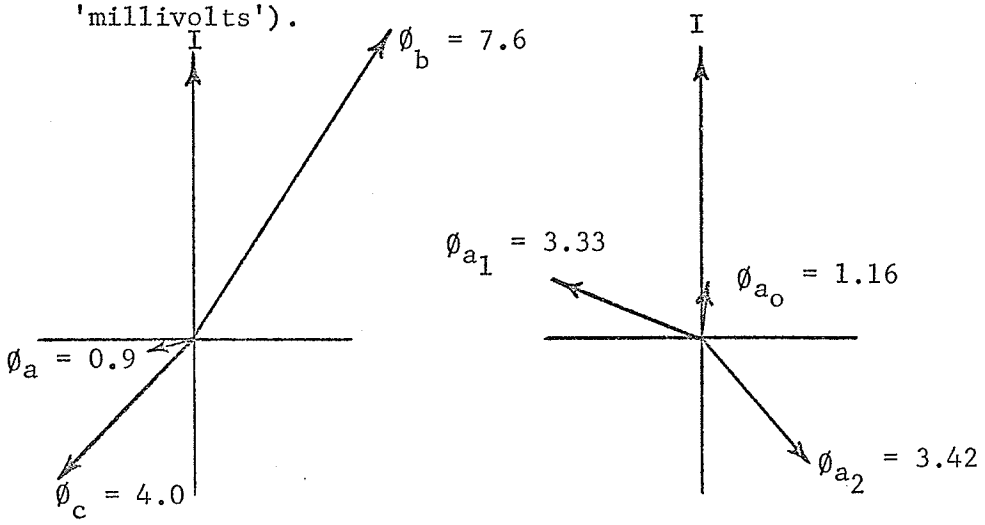

Figure 24b: CO-8 flux distribution at 300 Hz. (Relative magnitudes in 'millivolts').

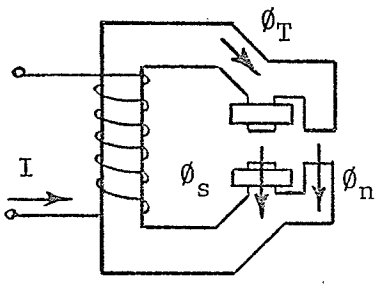

E.E. Co. type CDG13
Range 1.5 - 6 Amps
Tap = 2
I = 6 Amps

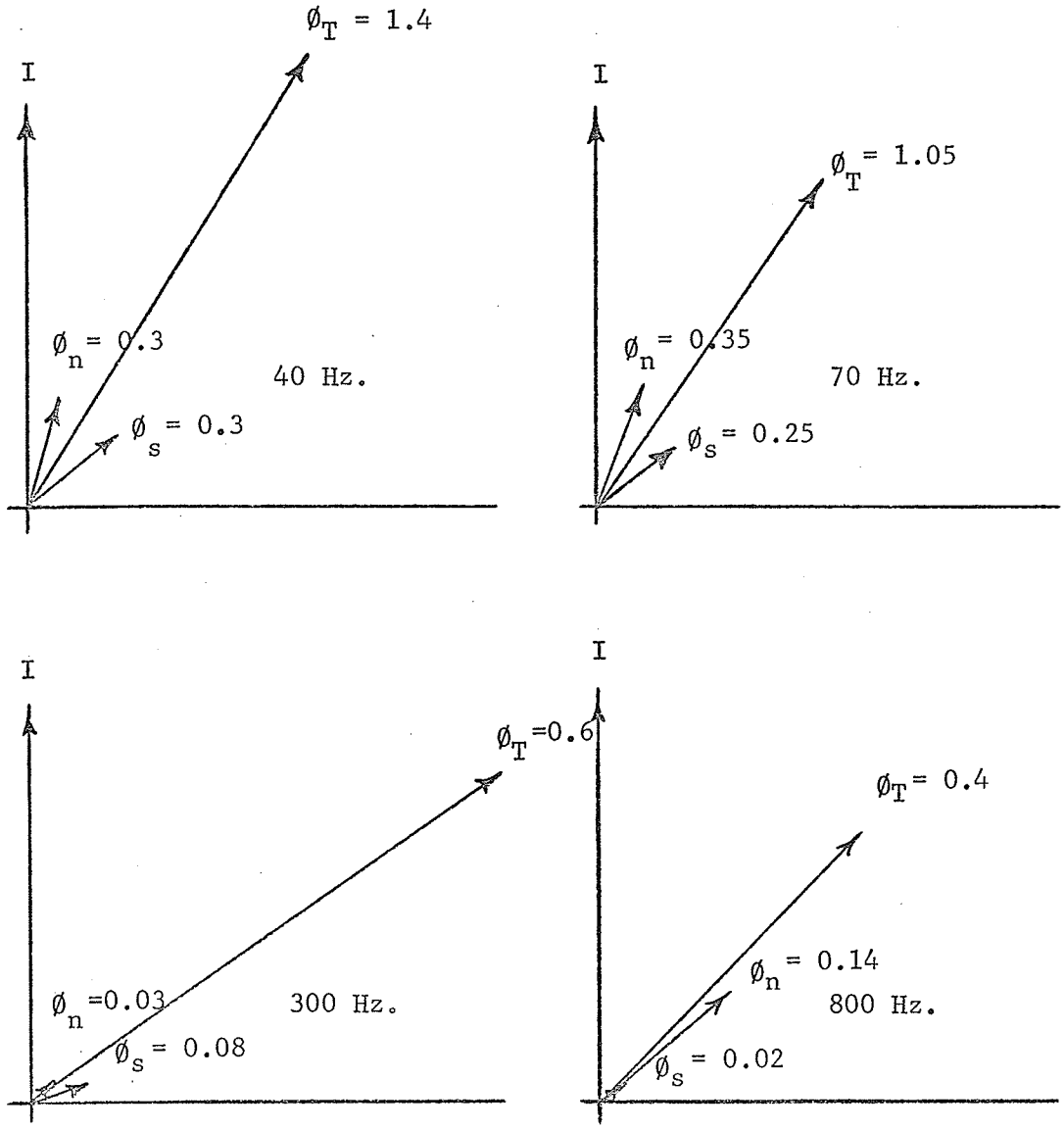

Figure 25: CDG13 air gap flux changes with frequency (Relative magnitudes in 'millivolts').

duced with increasing frequency. At approximately 800 Hz the fluxes were in phase and no net torque resulted. Above 800 Hz the direction of torque in the disk reversed.

5.3 Co-ordination With Torque Relations

The results obtained are seen to be in agreement with the principles of Figure 23. The increase in frequency produces effects on the electromagnet fluxes passing through the disk, the result of which is to change the manner in which they break down into positive and negative sequence components. When the negative sequence component takes precedence, the direction of torque produced within the disk reverses.

CHAPTER 6

CONCLUSIONS

1. Characteristics of induction-type protective relays are affected by harmonically distorted wave shapes.
2. Different relays are affected to different degrees by similar amounts of harmonic distortion in their operating wave shapes.
3. The degree to which a relay will be affected by harmonically distorted wave shapes is related to the frequency response characteristic of the relay.
4. At frequencies in the order of the design frequency and below, torque produced and therefore operating characteristics are directly proportional to frequency.
5. Higher frequencies including those in the harmonic range cause changes in the manner in which air gap fluxes break down into positive and negative sequence components. This effect can cause decreasing relay torque or actual reversal of relay torque to occur.

None of the effects encountered are severe enough to require reconsideration of the suitability of induction-type relay devices for conventional ac systems. Where incorporation of dc systems is involved, however, some caution is warranted in the selection of relay devices until such time as more practical knowledge is gained of the way in which the ac harmonics manifest themselves in the ac system.

It is suggested that the frequency response curve is the most accessible method of judging a relay's performance in this respect and would be a desirable addition to the published characteristics for relay devices.

BIBLIOGRAPHY

1. C. Adamson and N. G. Hingorani, 'High Voltage Direct Current Power Transmission', Garraway Ltd., June 1960.

2. B. J. Cory, 'High Voltage Direct Current Converters and Systems', MacDonald and Co., London, 1965.

3. Proceedings, Manitoba Power Conference, EHV-DC, Winnipeg, Canada, June 6-10, 1971.

4. Contributions, Conference on High Voltage D.C. Transmission, IEE Power Division, September 19-23, 1966.

5. C. Russel Mason, 'The Art and Science of Protective Relaying', John Wiley and Sons, Inc., 1956.

6. 'Protective Relays Application Guide', The English Electric Company Limited, Stafford, 1968.

7. M. A. Faucett and C. A. Keener, 'Harmonics May Delay Relay Operation', Electrical World, April 9, 1938.

8. A. R. van C. Warrington, 'Protective Relays', Chapman and Hall, 1962.

9. 'Applied Protective Relaying', Westinghouse Electric Corporation, Relay-Instrument Division, Newark, New Jersey.

10. C. A. Keener, M. A. Faucett, M. S. Helm, 'Magnetic Fields in Watt-Hour Meters', Transactions AIEE, May 1941.

11. W. E. Glassburn and W. K. Sonnemann, 'Principles of Induction Type Relay Design', Transactions AIEE, February 1953.

12. W. K. Sonnemann, 'A New Inverse Time Overcurrent Relay With Adjustable Characteristics', Transactions AIEE, February 1953.

13. H. H. Skilling, 'Electrical Engineering Circuits', John Wiley & Sons, Inc., 1960.

14. H. H. Skilling, 'Electromechanics, A First Course in Electromechanical Energy Conversion', John Wiley & Sons, Inc., 1962.

15. Publication MS/3018, 'Inverse Time Overcurrent Relays, Type CDG' The English Electric Company Limited, Meter, Relay & Instrument Division, Stafford.

APPENDIX A

HARMONIC CONTENT OF STATION AC WAVE FORMS

Measurements were taken at the Harrow Substation, Manitoba Hydro System, on December 13, 1969. In all measurements, a non-inductive resistance of 1.0 + j 0.0 ohm was inserted in the current transformer secondary circuit. The voltage drop across the resistance was measured with a Hewlett Packard model 302-A Wave Analyzer.

The frequency range examined was between 60 and 4000 Hz. Above 2100 Hz (35th harmonc), either no harmonic content existed, or was less than 70 to 80 db below the fundamental and could not be measured. All measurable harmonics were recorded and listed in the Tables which follow:

Table I - Transformer phase currents on the 115 kV side of Bank No. 9.

Table II - Transformer phase currents on the 24 kV side of Bank No. 9.

Table III - Transformer phase currents on the 115 kV side of Bank No. 3.

Table IV - Transformer phase currents on the 24 kV side of Bank No. 3.

Table V - Neutral currents on the 115 kV side of Banks 3, 4, 9 and 10.

Table VI - Ground currents in the 66 kV Ground Bank No. 3.

TABLE I

Transformer phase currents on the 115 kV side of Bank No. 9.

CT ratio = 300/5 (60/1)

Current In Primary of C.T.

Harmonic	(Milliamps)			(% of Fundamental)		
	AØ	BØ	CØ	AØ	BØ	CØ
1	52,800	54,000	51,600	100.0	100.0	100.0
2	48.0	30.0	45.0	0.091	0.055	0.087
3	528.0	600.0	960.0	1.0	1.1	1.86
4	30.0	24.0	12.0	0.057	0.044	0.023
5	960.0	960.0	960.0	1.82	1.78	1.86
7	540.0	480.0	540.0	1.02	0.89	1.05
9	12.0	12.0	12.0	0.023	0.022	0.023
10	nil	nil	6.0	nil	nil	0.012
11	138.0	90.0	78.0	0.262	0.167	0.151
13	78.0	90.0	60.0	0.148	0.167	0.116
15	3.6	nil	4.8	0.007	nil	0.009
17	18.0	20.4	13.2	0.033	0.038	0.025
23	8.4	8.4	6.0	0.016	0.016	0.012
25	2.4	nil	nil	0.005	nil	nil
35	3.6	6.0	6.0	0.007	0.011	0.012

TABLE II

Transformer phase currents on the 24 kV side of Bank No. 9.

CT ratio = 300/5 (60/1)

Current In Primary of C.T.

Harmonic	(Milliamps)			(% of Fundamental)		
	AØ	BØ	CØ	AØ	BØ	CØ
1	69,000	72,000	69,000	100.0	100.0	100.0
2	nil	108.0	84.0	nil	0.150	0.120
3	600.0	840.0	960.0	0.869	1.17	1.39
4	30.0	36.0	48.0	0.043	0.050	0.069
5	1830	1740	1770	2.65	2.42	2.57
7	300.0	312.0	312.0	0.435	0.433	0.600
8	18.0	24.0	nil	0.026	0.033	nil
9	42.0	36.0	78.0	0.061	0.050	0.113
10	18.0	nil	nil	0.026	nil	nil
11	198.0	210.0	204.0	0.287	0.292	0.296
13	138.0	180.0	162.0	0.200	0.225	0.235
17	30.0	30.0	nil	0.043	0.042	nil

TABLE III

Transformer phase currents on the 115 kV side of Bank No. 3.

CT ratio = 300/5 (60/1)

Current In Primary of C.T.

Harmonic	(Milliamps)			(% of Fundamental)		
	AØ	BØ	CØ	AØ	BØ	CØ
1	72,000	78,000	75,600	100.0	100.0	100.0
2	24.0	45.0	30.0	0.03	0.058	0.040
3	280.0	600.0	168.0	0.389	0.770	0.222
5	1230	1170	1440	1.71	1.50	1.90
7	600.0	660	672	0.834	0.846	0.886
9	48.0	48.0	42.0	0.067	0.062	0.056
11	30.0	30.0	30.0	0.042	0.038	0.040
13	66.0	78.0	72.0	0.092	0.10	0.095

TABLE IV

Transformer phase currents on the 24 kV side of Bank No. 3.

CT ratio = 1000/5 (200/1)

Current In Primary of C.T.

Harmonic	(Milliamps)			(% of Fundamental)		
	AØ	BØ	CØ	AØ	BØ	CØ
1	368,000	366,000	366,000	100.0	100.0	100.0
2	300.0	60.0	150.0	0.082	0.016	0.041
3	460.0	1,400	800.0	0.125	0.382	0.218
4	100.0	100.0	nil	0.027	0.027	nil
5	5,600	8,300	8,600	1.52	2.26	2.35
6	nil	100.0	nil	nil	0.027	nil
7	3,000	5,600	5,600	0.815	1.53	1.53
8	100.0	100.0	100.0	0.027	0.027	0.027
9	140.0	400.0	350.0	0.038	0.109	0.096
11	460.0	300.0	900.0	0.125	0.082	0.245
13	300.0	300.0	680.0	0.082	0.082	0.186
15	nil	100.0	nil	nil	0.027	nil
17	240.0	300.0	nil	0.085	0.082	nil

TABLE V

Neutral currents in the 115 kV side of Banks 3, 4, 9 and 10.

CT ratio = 200/5 (40/1)

Harmonic	Current In Primary of C.T. (Milliamps)	(% of Fundamental)
1	4,800	100.0
2	29.0	0.605
3	1,680	35.0
4	16.0	0.334
5	76.0	1.58
6	4.8	0.10
7	27.2	0.566
9	108.0	2.25
11	7.2	0.15
13	5.6	0.117
15	21.6	0.45
21	4.0	0.083

TABLE VI

Ground currents in the 66 kV Ground Bank No. 9.

CT ratio = 600/5 (120/1)

Harmonic	Current In Primary of C.T. (Milliamps)	(% of Fundamental)
1	1,320	100.0
2	45.6	3.46
3	709.0	53.7
4	24.0	1.82
5	312.0	23.6
6	27.6	2.09
7	38.4	2.91
9	60.0	4.54
11	40.8	3.09
13	12.0	0.91
15	12.0	0.91

APPENDIX B

TYPICAL AC SYSTEM FAULT WAVE FORMS

OSCILLOGRAPH I - Parkdale Station
Feb. 4, 1970
Line H-18 Skywire hit by aircraft

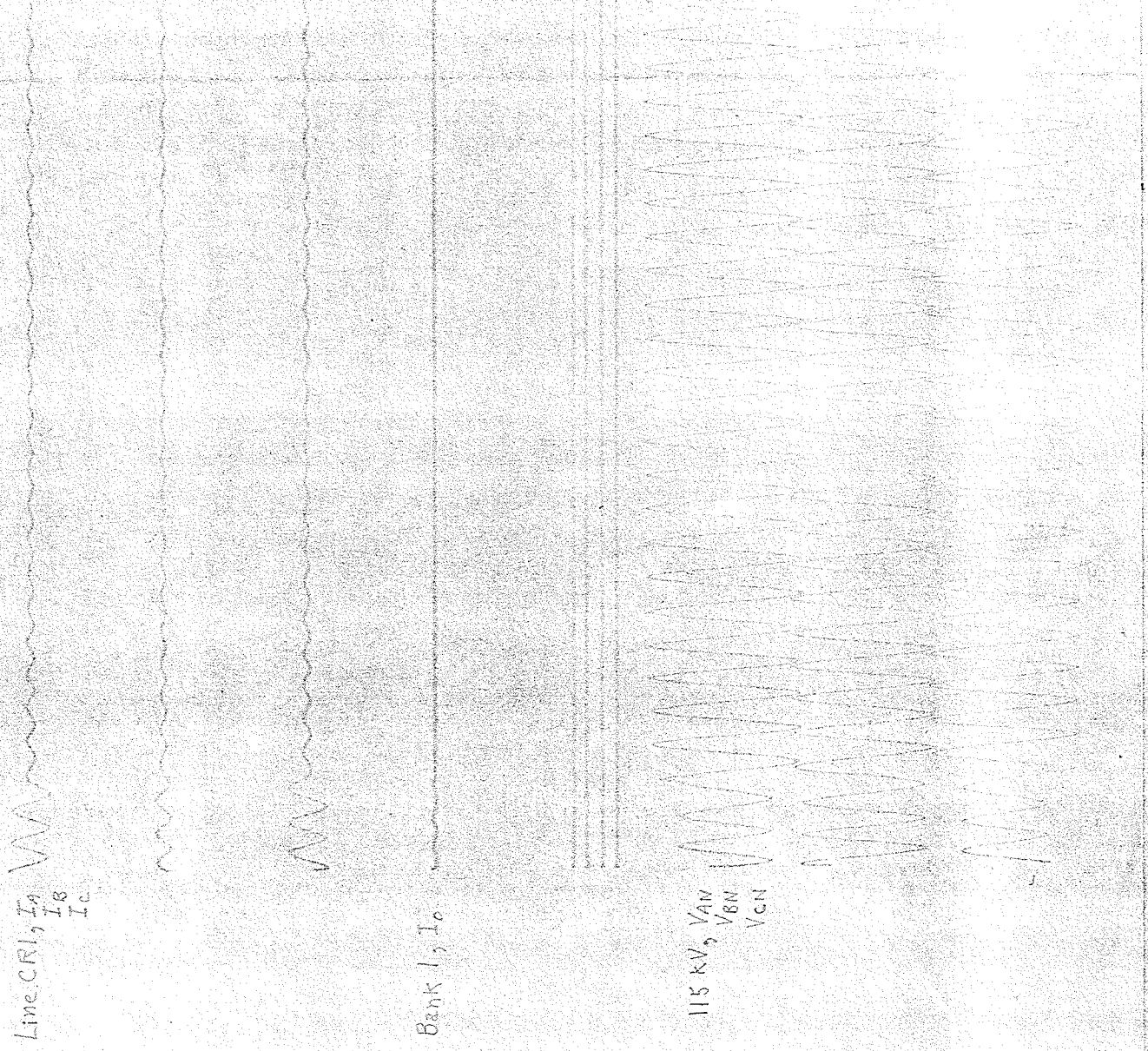

OSCILLOGRAPH II - Rosser Station
July 12, 1969
R5C line fault

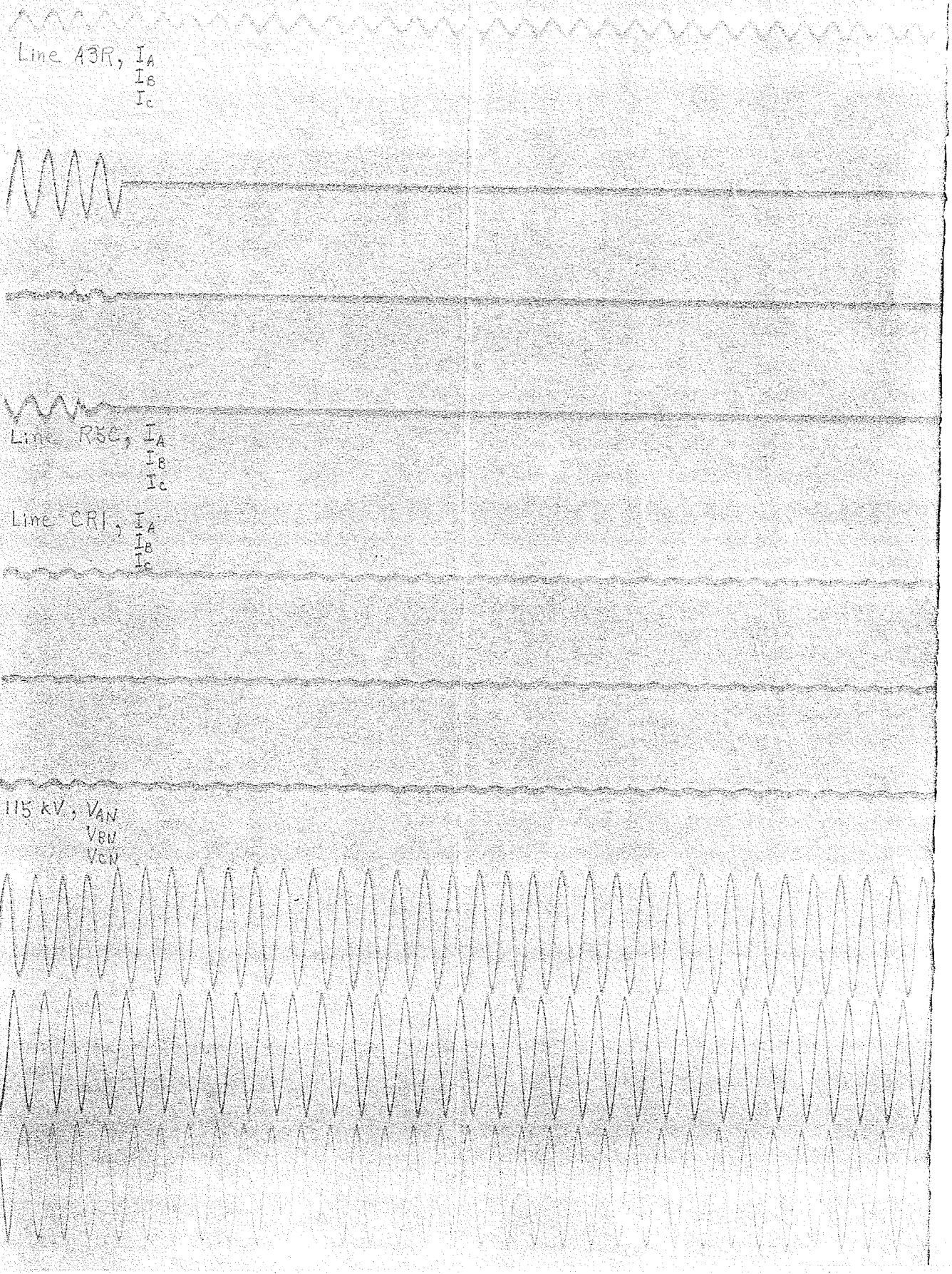

OSCILLOGRAPH III - Transcona Station
Dec. 5, 1968
TM1 line fault

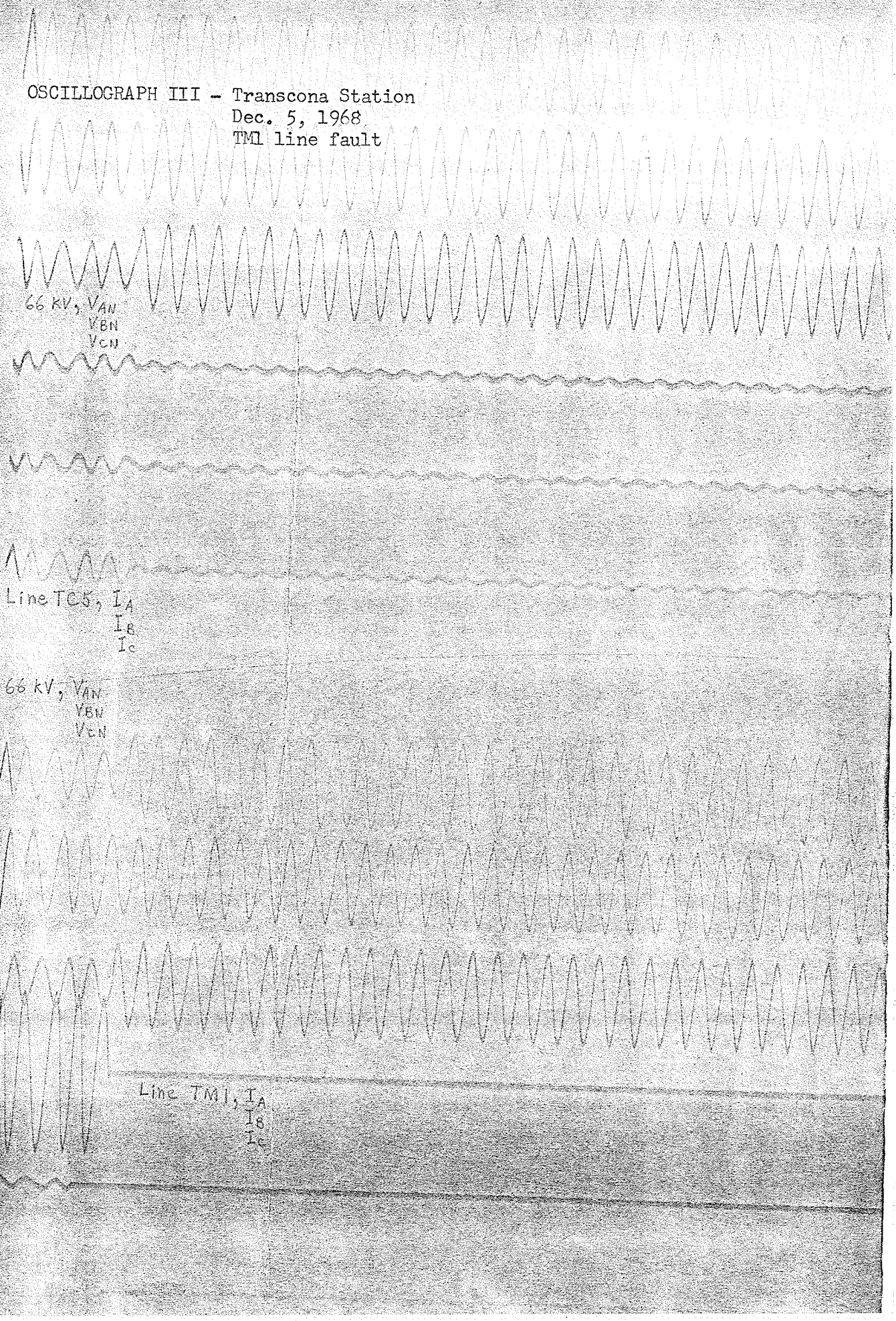

OSCILLOGRAPH IV - Transcona Station
June 26, 1969
Amy St. bus fault